Climate Services 34 (2024) 100487

Contents lists available at ScienceDirect

Climate Services

journal homepage: www.elsevier.com/locate/cliser

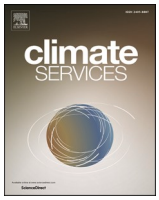

Original research article

The digital climate atlas of the Canary Islands: A tool to improve knowledge of climate and temperature and precipitation trends in the Atlantic islands

Ángel L Luque Söllheim [a,b,*], Pablo Máyer Suarez [c], Fabián García Hernández [d]

[a] Institute for Environmental Studies and Natural Resources (i-UNAT), University of Las Palmas de Gran Canaria, Spain
[b] Edificio de Ciencias Básicas - Campus de Tafira, 35017, Las Palmas de Gran Canaria, Spain
[c] Geography, Environment and Geographical Information Technologies Group (GEOTIGMA), The Oceanography and Global Change Institute (IOCAG), University of Las Palmas de Gran Canaria, Spain
[d] Tragsatec S.A., Empresa de Transformación Agraria, S.A, Spain

ARTICLE INFO

Keywords:
Climate atlas
Climate data series
Climate mapping
Decadal trends
Köppen

ABSTRACT

This paper presents the Interactive Digital Climate Atlas of the Canary Islands, a web portal based on geographic information systems for the dissemination of climate information. It provides citizens and public and private administrations with high spatial resolution maps (100 m) of different climate variables such as temperature, rainfall, relative humidity, cloudiness frequency and wind velocity. Also available are Köppen climate classification maps and decadal trends of temperature and precipitation in a context of climate change. This spatial resolution is suitable for the detailed climatic description of small and orographically complex islands. For this purpose, climate series from databases of different public institutions as well as data from remote sensing and reanalysis systems were employed. A statistical process involving data filtering and the detection and correction of inhomogeneous segments was carried out as a preparatory step. Then, a spatial interpolation model was developed using a multiple linear regression method for the generation of the high spatial resolution climate cartography. The results are annual and monthly maps of the climate variables in Canary Islands at 100 m spatial resolution and with different time periods depending on the availability of data on the different variables, but in most cases between 1991 and 2020. Following the European Directive INSPIRE (Directive 2007/2/CE, Infrastructure for Spatial Information in Europe), both map visualisation and downloading in GeoTIFF and NetCDF format are permitted, as well as consultation of the data and metadata of the climatic series used.

Practical implications

The unique peculiarities of the climate of the Canary Islands are the result of a specific combination of regional atmospheric conditions and geographical factors. Climate analyses of the islands that are not undertaken at zonal, regional and local scales run the risk of making serious errors. At zonal scale, consideration can be given to the latitude at which the archipelago is located (28°N), to the climatic repercussions of its proximity to the large warm surface of the African continent, and to the impact of the cold marine current of the Canary Islands. At regional scale, it is possible to take into account the fragmented nature of the Canary Islands territory, which is made up of a group of islands and islets totalling 7,474 km2. Finally, at local scale, the specific orographic features of each of the islands can be incorporated, along with the different altitudes and orientations of their reliefs which introduce highly significant climatic differences not only between the islands themselves but even between slopes of the same island.

The above allows us to frame the objective of the work presented here: the creation of a Digital Climate Atlas of the Canary Islands that incorporates, on the one hand, the impact of the variations in altitude and orientation of the island reliefs on different climatic variables –and the consequent generation of multiple topoclimates- and, on the other, a specific section that shows the decadal trends of precipitation and air temperature.

This work is part of a set of measures undertaken by different Spanish state, regional and local administration bodies aimed at disseminating information about the climate and, most importantly, climate change. In this context, the present work is the

* Corresponding author.
E-mail addresses: angel.luquesolheim@ulpgc.es (Á.L. Luque Söllheim), pablo.mayer@ulpgc.es (P. Máyer Suarez).

https://doi.org/10.1016/j.cliser.2024.100487
Received 17 April 2023; Received in revised form 15 March 2024; Accepted 2 May 2024
Available online 23 May 2024

result of a collaboration between the regional administration (Department of Ecological Transition, Fight against Climate Change, and Territorial Planning of the Government of the Canary Islands), the University of Las Palmas de Gran Canaria and the company Cartográfica de Canarias S.A. (GRAFCAN). It is a GIS-based web portal for the dissemination of climate information of the Canary Islands archipelago. High spatial resolution maps (100 m) of different climatic variables are made available to citizens and public and private administrations. These variables (monthly and annual mean values are represented) include temperature (mean, maximum and minimum), precipitation, humidity, cloud frequency and wind speed. Also included are detailed Köppen climate classification maps and maps of decadal trends in temperature and precipitation.

For this purpose, climatic series were used from the databases of different public institutions, including the Spanish Meteorological Agency (AEMET by its initials in Spanish), Spain's Agroclimatic Information Network for Irrigation (SIAR by its initials in Spanish), and the Island Councils of La Palma, Tenerife, Gran Canaria, Fuerteventura and Lanzarote, as well as data obtained from remote sensing and reanalysis systems.

A statistical process of data filtering and homogenization has been carried out, followed by the application of a spatial interpolation model based on observations of the homogenized meteorological stations and reanalysis points for the generation of the climate cartography. Following the European Directive INSPIRE (2007), it is possible to view and download maps in GeoTIFF and NetCDF format (https://atlasclimatico.sitcan.es: last accessed March 2024), as well as to consult the data and metadata of the climatic series used.

It comprises a useful tool for works that require the use of climatic data and facilitates an understanding of the evolution of temperature and precipitation and the trends in the series. It is also a very useful teaching resource, providing detailed information about the main types of climate in the Canary Islands, and enabling consultation of data series of the different variables in any part of the territory as well as information about these series (source, time periods, data characteristics, etc.).

In the coming years it will be essential to continue expanding and improving this portal, including the English version, with updates that incorporate new climate series from new observation networks and satellite systems. Also of fundamental importance will be the incorporation of multiple indicators related to climate change and, as a key element, the projections of climate change scenarios at high spatial resolution, based on the Sixth Assessment Report of the IPCC.

The web portal can be accessed via the following link: https://www.gobiernodecanarias.org/cambioclimatico/materias/sistemas-observacion and directly at https://atlasclimatico.sitcan.es.

1. Introduction

In recent decades, more and more public and private administrations and companies, as well as citizens in general, have been demanding climate information. Proof of this is the growing public investment in products of all kinds based on climate parameters. These include climate databases, products derived from satellite analysis and tools enabling the visualisation and downloading of climate data, especially in relation to climate change. Digital atlases are one of the tools that have proven to be effective for the visualisation and dissemination of various climate parameters, as well as climate change. These show general aspects of different climate variables, information about which should be easily accessible in compliance with the Directive INSPIRE (2007).

In general, digital atlases providing global coverage tend to have spatial resolutions of 50 to 5 km, as described by Harris et al. (2014). Initially these were at 50 km resolution, but were subsequently reduced to 21 km resolution, as described by Fick and Hijmans, (2017), using 1960–2018 data series to generate the accessible WorldClim global climate and weather data maps. Also noteworthy is the Intergovernmental Panel on Climate Change (IPCC) atlas which contains maps of global temperatures, rainfall and trends at about 25 km resolution, as described by Iturbide et al. (2021). While these atlases offer good descriptions of climate and its changes over large plains, deserts and continental basins, this is not the case for small mountain systems in general or islands of complex orography. Other atlases have a higher spatial resolution but cover periods prior to the recent climate period (1991–2020). These include, among others, a 1 km spatial resolution atlas described by Fick and Hijmans (2017) covering the 1970–2000 period and the Digital Climate Atlas of Mexico, with a spatial resolution of 926 m and daily data for the period 1902–2011, as described by Fernández et al. (2014). Others have focused on specific islands or regions, including the Climate Atlas of Hawaii described by Giambelluca et al. (2014), and the Digital Climate Atlas of the Iberian Peninsula by Ninyerola et al. (2005), which show maps of climate variables at resolutions between 200 and 300 m. Although these are useful spatial resolutions for regions of complex orography, the latter does not cover the Canary archipelago. Finally, the closest atlas to the present work is the climate atlas of the archipelagos of the Canary Islands, Madeira and the Azores (AEMET, 2012). It shows mean maps of temperature and precipitation at 100 m resolution in the Canary Islands, but for the earlier period of 1971 to 2000 and without a digital web facility.

In this context, the main aim of the present paper is to detail the methodology used to generate the Interactive Digital Climate Atlas of the Canary Islands (ACDIC by its initials in Spanish), as well as the results obtained from it with examples that allow the user to interpret the maps correctly. It is a useful tool for accessing maps of different climatic variables. Its spatial resolution of 100 m allows interpretation of the topoclimatic nuances present in each of the islands (Marzol and Máyer, 2012), and its databases of different climate parameters are available for download on the web. In addition, the Atlas includes Köppen climate classification (Kottek et al., 2006) and decadal temperature and precipitation trend maps, useful in a context of global climate change. In the same line as other atlases (Antolović et al., 2013), the ACDIC is designed as a Web-GIS (Geographic Information System) application with texts describing the Canary Islands climate and different tools for map visualization, charts of climate variables, metadata of the series (https://atlasclimatico.sitcan.es/) and the option to download images in GeoTIFF and NetCDF format, in compliance with the Directive INSPIRE (2007) (https://opendata.sitcan.es/). The management and maintenance of the website is the responsibility of the public company GRAFCAN, SA, which is owned by the Government of the Canary Islands. The Government has committed to maintaining and updating the contents of this website.

2. Some characteristics of the Canary Islands

The Canary Islands is an archipelago made up of a group of islands and islets totalling 7,474 km^2, located between 27.64°N and 29.42°N and −13.33°W and −18.16°W in the Atlantic Ocean and approximately 100 km off the northwest coast of the African continent (Fig. 1). As indicated by Marzol and Máyer (2012), this archipelago is located in the transition zone between the temperate and the tropical world, which gives its atmosphere similar characteristics to those of other areas such as the coasts of California, Chile and Peru in the Pacific Ocean or those of South Africa and Namibia in the South Atlantic, all of which are immersed in the air flows associated with subtropical high pressure systems: in the case of the Canary Islands, the Azores anticyclone. Among the factors that generate climatic diversity is the existence of a thermal inversion at around 1,000 m altitude that separates a surface layer of air, of higher turbidity and in which the winds of the first quadrant predominate, and an upper layer of air, in which the winds of the third quadrant predominate (Marzol and Máyer, 2012). As a result of

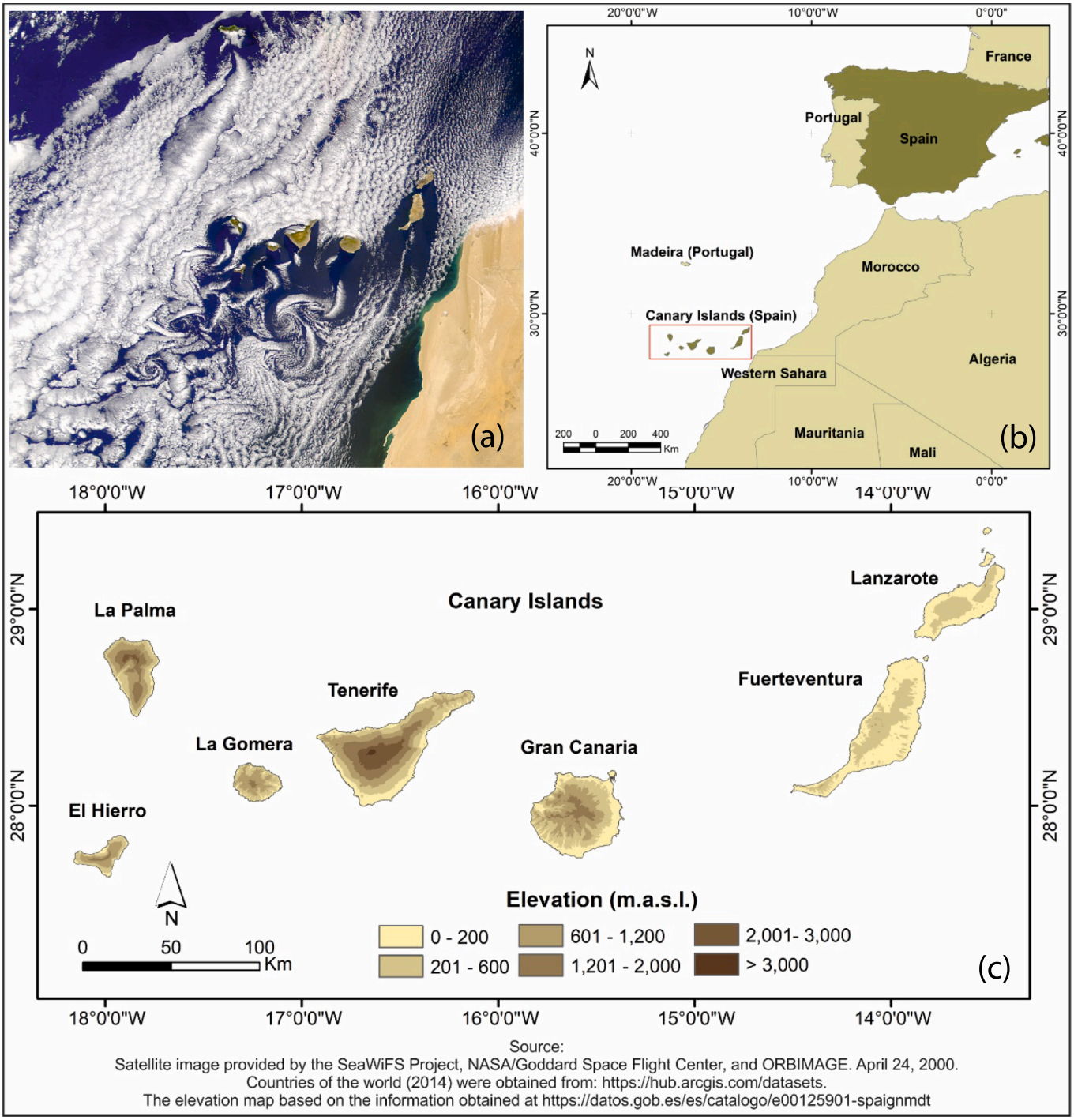

Fig. 1. (a) Recent satellite image of the Canary Island area showing a common trade winds day and cloud distribution. (b) Location of the Canary Archipelago in the Atlantic Ocean. (c) Position on scale, names of the islands and elevation map.

the high visibility of the latter, one of the most important astronomical observatories in Europe has been installed on the island of La Palma and others, also of note, on the island of Tenerife. This thermal inversion, which varies between an altitude of around 600 m in summer and 1,700 m in winter (Dorta Antequera, 1996), has repercussions for wind direction, humidity and, in particular, cloudiness, as it prevents the vertical growth of clouds and, therefore, the generation of precipitation. This stratiform cloudiness is blocked by the northern slopes of the islands whose reliefs exceed the height of the inversion, generating landscapes of enormous contrast, especially between northern and southern slopes. The climatic diversity of this archipelago, therefore, stems from this peculiar structure of the atmosphere, to which other equally important factors can be added, such as: (i) its proximity to the African continent, with the consequent advection of Saharan air, warm and dry in summer, cold in winter and generally accompanied by suspended dust; (ii) the existence of a cold marine current (the Canary Current), which is colder the closer it is to the African continent; and (iii) the steep orography of the islands, especially the westernmost islands (with a maximum altitude of 3,718 m at the peak of Teide on the island of Tenerife). All these factors generate significant modifications to different climate variables and, at the same time, a diversity of topoclimates, which we have tried to capture in the Digital Climate Atlas

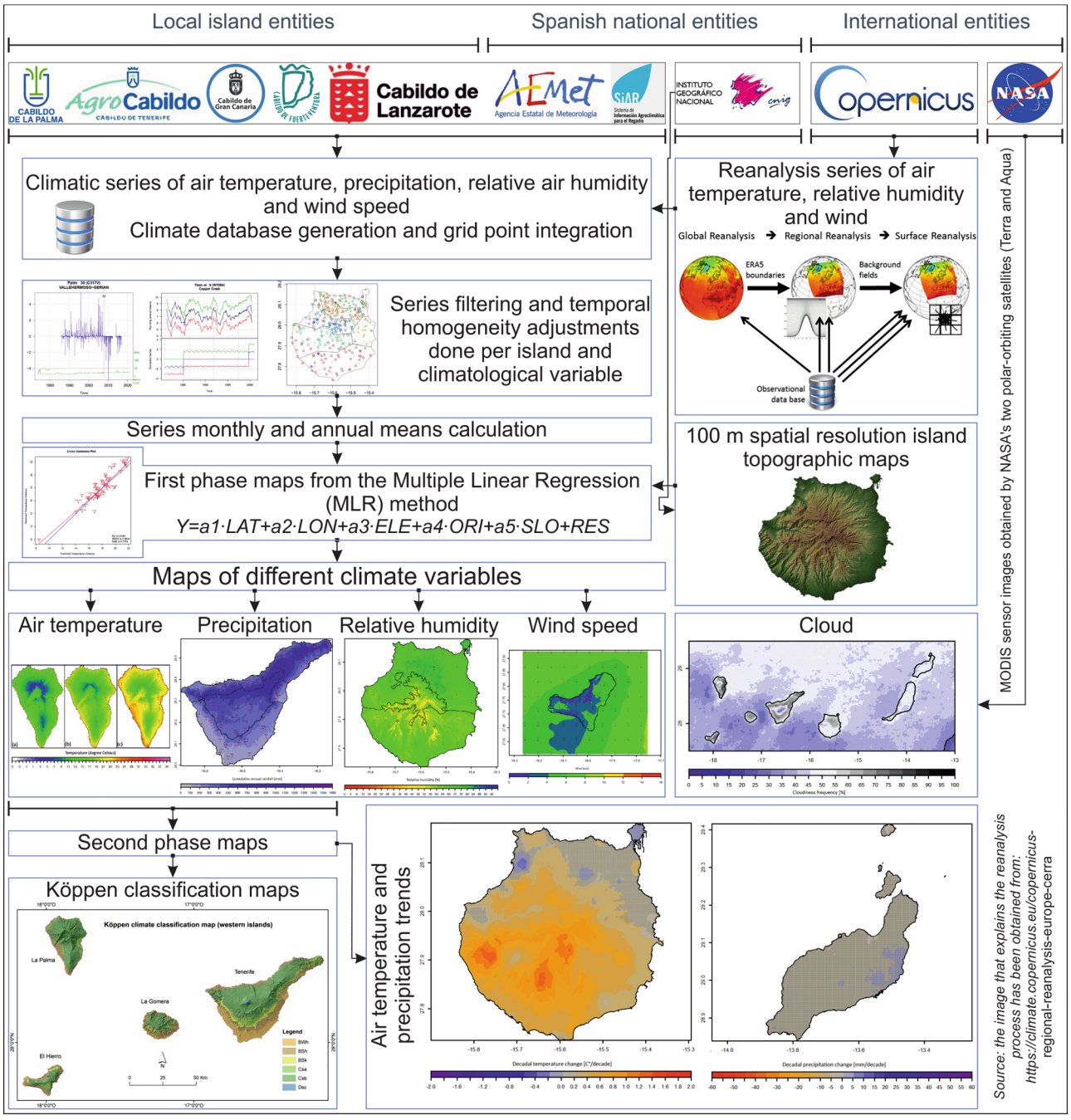

Fig. 2. Data series processing scheme and climatological maps generation methodology.

presented here.

Below, a description is given of the methodology employed to generate the different products shown in the Atlas, A flowchart is also provided (Fig. 2), summarizing the data used and the methodological process.

3. Data and methodology

3.1. Data sources

Observational data for the last 50 years (1970–2020) were acquired from networks managed by competent national and regional bodies, including the Spanish Meteorological Agency (AEMET by its initials in Spanish), Spain's Agroclimatic Information Network for Irrigation (SIAR by its initials in Spanish), and the Island Councils of La Palma, Tenerife, Gran Canaria, Fuerteventura and Lanzarote (Table 1). ERA5-Land and UERRA MESCAN-SURFEX reanalysis data generated by the ECMWF (European Centre for Medium-Range Weather Forecasts) at 9 and 5.5 km spatial resolution and described by Muñoz Sabater (2019) and Copernicus a (2019), respectively. In the case of wind speed also UERRA HARMONIE reanalysis data at different pressure levels. They were also acquired from the Copernicus web portal (Copernicus b, 2019).

The series of minimum, maximum and mean air temperatures recorded at each meteorological station were provided by the institutions in charge of the measurement networks (Table 1). The original series dated back to pre-1970, but only the recent period from 1991 to 2020 was processed. To fill data gaps in areas with very few stations, ERA5-Land reanalysis points were incorporated. The precipitation series

Table 1
Number of used series in the atlas per island, climatological parameter, data periods and data.

Variable	Period	Origin of the data	ISLAND							
			La Palma	La Gomera	El Hierro	Tenerife	Gran Canaria	Fuerteventura	Lanzarote	Total
Air Temperature (°C)	1991–2020	AEMET	36	34	24	120	68	16	15	313
		Island Council	17	0	0	56	0	0	0	73
		SIAR	6	2	1	9	6	2	8	34
		Era 5-Land	6	2	3	9	7	5	7	39
Precipitation (mm)	1970–2020	AEMET	123	105	62	388	196	32	35	941
		Island Council	18	0	0	57	318	50	49	492
		SIAR	6	2	1	9	6	2	8	34
Relative humidity (%)	1991–2020	AEMET	23	11	13	74	25	11	8	165
		Island Council	17	0	0	50	0	0	0	73
		SIAR	6	2	1	9	6	2	8	34
		UERRA MESCAN-SURFEX	16	7	3	3	20	16	13	78
Wind speed (m/s)	2001–2020	AEMET	8	8	7	23	31	8	9	94
		Island Council	0	0	0	56	0	0	0	56
		SIAR	6	2	1	9	6	2	7	33
		UERRA-HARMONIE	19	13	7	13	15	4	0	71
		UERRA MESCAN-SURFEX	136	87	72	200	183	271	198	1144
Cloudiness (frequency %)	2000–2014	MODIS sensor: 1 km resolution	Processed and remapped mean monthly and annual cloudiness frequency to the entire area of the Canary Islands, including the maritime zones, between −18.5° and −13° longitude and between 27.5° and 29.5° latitude at a spatial resolution of 400x400 m, 1320 grid points horizontally and 480 grid points vertically, that is a total of 633,600 points.							

used to generate the maps were of monthly accumulation in mm. The data range period to obtain the monthly and annual cumulative means was from 1970 to 2020 (Table 1), ensuring robust mean maps given the highly variable character of precipitation in these islands. However, in various western islands (El Hierro, La Palma and Tenerife) the series began in 1975 and in La Gomera in 1980. Precipitation is measured through a dense network of stations on the islands, and it was not necessary to add reanalysis grid points. The hygrometric information, in units of relative humidity in %, was taken from a total of 140 stations distributed unevenly across the islands for the recent period from 1991 to 2020 (Table 1). Due to the low numbers of series in all the islands (except Tenerife thanks to the AGROCABILDO network), it was decided to incorporate grid points with 2 m relative humidity data from the UERRA reanalysis system (MESCAN-SURFEX). It was found that a greater spatial resolution of the reanalysis data (5.5 km instead of the 9 km of ERA-Land) was an important factor to obtain closer to real relative humidity in the more mountainous islands. In the case of wind, the processed period was shorter, from 2001 to 2020, due to the scarcity of wind stations in the islands (Table 1). Map development focused on wind speed, not direction, because in the Canary Islands, on average, N-NE trade winds predominate throughout the year. Winds in coastal waters and in the inter-island channels, areas with very few observations in general, are important. For this reason, reanalysis MESCAN-SURFEX data were incorporated in this variable. As few wind observations were available in high altitude island areas, UERRA-HARMONIE grid points were added. These are not surface data but are based on pressure level layers to reach as near as possible real altitudes in the peak areas of each island. With respect to cloudiness, this variable has only been measured at the 8 existing airports in the Canary Islands since the beginning of air operations in the 1960 s to 1980 s. Therefore, the cloudiness parameter was processed by using remote sensing techniques from the Modis sensor at 1 km spatial resolution and between 2001 and 2014 (Table 1).

3.2. Methodology

Monthly time series data obtained from the observations of the measurement stations were subjected to control and correction processes to debug errors and correct inhomogeneities before final interpolation and map generation. The methodology process is summarized in the flowchart shown in Fig. 2. It can be seen that there are two main phases after data acquisition and time series processing: a first phase involving the generation of basic maps of temperature, precipitation, relative humidity, wind speed, and cloudiness, and a second phase based on Köppen classification maps and the generation of trend maps. The following are the main processes that were carried out.

3.2.1. Series filtering.

All data series were subjected to a detailed analysis with filtering of those with fewer than 5 complete years. This threshold was varied depending on the number of data series available for each parameter and taking into account its variability (7 years for temperature and relative humidity, 15 for precipitation and 5 for wind). The filter used depended on the percentage of the temporal range of the data. If the range of the series was 50 years for precipitation (1970–2020), those series with less than 15 years of data were eliminated in order to impact the mean values as little as possible. That is, leaving series with a data quantity greater than 25 % to 30 % of the study period. This threshold may be debatable in areas with very irregular precipitations such as those in the south-western slopes of the mountainous islands, as well as in high areas above the inversion level. Following the procedure of Raso (1984), an indirect way of expressing the interannual variability of precipitation is to determine the ideal value of the number of years n necessary to obtain adequate statistical confidence levels. This is obtained from the following statistical equation (1):

$$n = \frac{Z^2 \sigma^2}{e^2} \quad (1)$$

where n is the number of years, Z is the standardized variable that follows the normal distribution law and takes values of 1.65, 1.96 and 2.58 for 90 %, 95 % and 99 % statistical significance respectively, σ is the variance of the time series, and e is the error in the arithmetic mean, which was taken as 10 %. In this sense, statistically speaking, series with a length of between 30 and 60 years would be needed to obtain a 90 % confidence interval for the means and of between 80 and 160 years for a 99 % confidence interval. In the latter case, there would not have been enough precipitation series to characterize this variable, especially in the western islands (La Palma, El Hierro, La Gomera and Tenerife) which had a low number of precipitation series for the years 1970 to 1980. For this reason, the minimum size of the precipitation series was set at 15 years, making the average temporal range of the precipitation series in the islands at about 37 years and hence enabling at least a 90 % confidence interval. In the case of the other variables where the variance is much lower, the percentage was maintained at around 25 %-30 % according to the studied period. Thus, for example, in the cases of

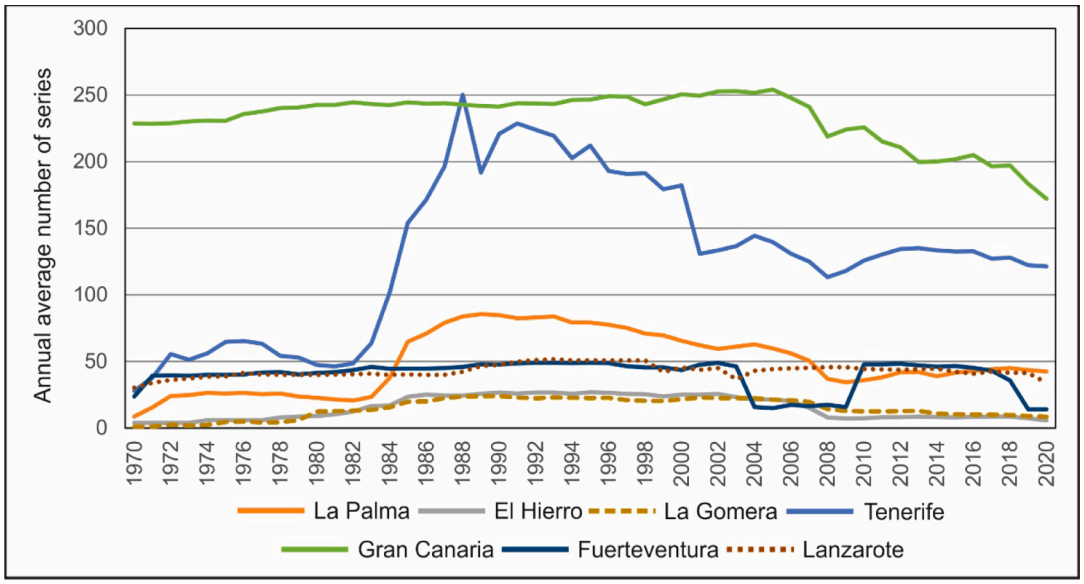

Fig. 3. Annual average number of precipitation series in the Canary Archipelago from 1970 to 2020.

temperature and relative humidity with a period of 30 years (1991–2020), the filter was set at 7 complete years with monthly data. Applying the same criterion as with precipitation (Raso, 1984) to the series of average air temperature with less variability, 4 years would be sufficient to obtain a 99 % confidence interval for the means. In the case of wind with a study period established at 20 years (2001–2020), the filter was set at 5 years (25 %).

A search was conducted to detect errors with extreme values that exceeded the statistical thresholds established on the basis of the data of the series itself and when these appeared in isolation with no reflection in the other data series of the network. Such data were therefore considered not to be related to the climate but to measuring anomalies of the observation station in question. The third step was to obtain small missing data by cross-correlation (greater than 0.86) with neighbouring data series.

3.2.2. *Temporal homogeneity adjustments*

Jumps in the mean from long data segments in individual series are detected and corrected by comparing them with series from their surroundings at the same segment time. Therefore, these anomalies are interpreted as being due to incidences that occurred during the measurement process at the observation station, not related to changes in the climate. Changes in the station's location, sensor calibration drift in time or negligence in station maintenance, among other factors, can cause these inhomogeneities in the data series. For this process, the *climatol* software application was used, available as an R package (Guijarro, 2023). This semi-automatic data processing software was designed for the iterative analysis of large networks of daily and/or monthly data. It analyses each series in temporal segments, computing the SNHT (standard normal homogeneity test) and obtaining the breaking points caused by probable inhomogeneities in the series. The test based on the SNHT index defined by Alexandersson (1986) is a dimensionless measure that allows the evaluation of the difference between the means of two subsets of the same time series. Once the inhomogeneity is detected, the software proposes several solutions to correct it, for example: a) taking as a basis the solution that minimizes the total final value of the SNHT of the series; b) minimizing the RMSE (root mean squared error) with respect to the environment's average; or c) adjusting only the shorter of the two homogenous sections before and after the jump in the mean. In any case, the user's supervision and review are always required to select the best solution in each case. We have tried to modify the original data as little as possible in the prior filtering process and in this homogeneity adjustment, which is why option c) was applied as the gentlest option for correcting the most evident inhomogeneities.

The procedure to determine an SNHT threshold that separates homogeneous series from series with possible inhomogeneous cuts was applied to each climatic variable on each island separately. Although previous works have predefined different SNHT thresholds for different levels of statistical significance and numbers of series (Alexandersson, 1986; Khaliq and Ouarda, 2007), these thresholds depend on the climatic variable itself, the temporal resolution of the variable, and even the geographic characteristics of the area of study (Guijarro et al., 2023), meaning that they need to be determined in each case. In a preliminary diagnosis, the *climatol* application computes anomaly graphs for the location of each series. The anomaly is the data series minus the expected location data, interpolated from the series of its environment. Inspection of these anomaly graphs allows the establishment of an initial range of SNHT values of the network considered as inhomogeneous. A second type of graph that the software provides in the diagnostic phase is a histogram of the maximum SNHT values obtained for the introduced series. Those frequencies ordered by the SNHT values and considered inhomogeneous are differentiated at the end of the histogram and accumulated in one or more secondary maxima. The beginning of the first secondary maximum in the histogram with SNHT values already defined as inhomogeneous from the anomaly graphs allows establishment of the SNHT threshold of the network. However, since this methodology is not exempt from subjectivity, as a final check the percentage of series affected by inhomogeneous cuts was obtained and it was determined that they should not exceed 30 % of the total series of the network. In the case of the air temperature series, the SNHT threshold was set at between 40 and 45 depending on the island, with inhomogeneous jumps affecting 20 % of the network series. The threshold was set at 20 in the case of monthly precipitation, affecting just under 15 % of the network series and in the case of relative humidity, at 35, showing inhomogeneous cuts in just under 30 % of the series. Finally, in the case of wind, the SNHT threshold varied between 15 and 30 depending on the island and affected 17 % of the series.

3.2.3. *Spatial interpolation*

There are several statistical-topographic methods to predict climatic variables continuously in areas where there are no meteorological stations. In this regard, the scientific literature focuses to a large extent on mountainous areas (Prudhomme and Reed, 1998, Goovaerts, 1999) because a complicated topography generates an extensive variety of

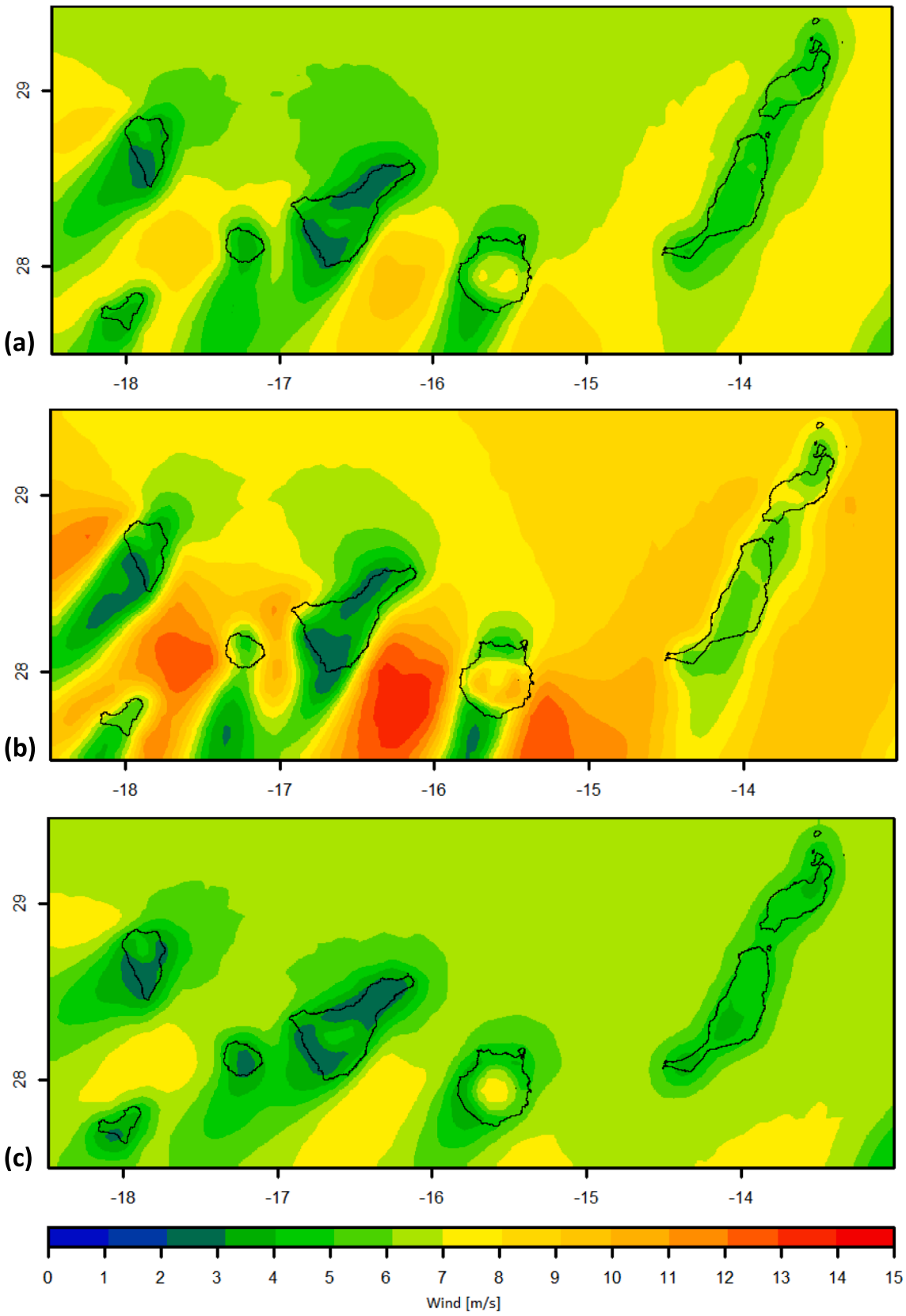

Fig. 4. Wind obtained from UERRA data for the Canary Archipelago in m/s, averaged for the period 2001–2020 at 400 m resolution. (a) Annual average, (b) July average, and (c) January average.

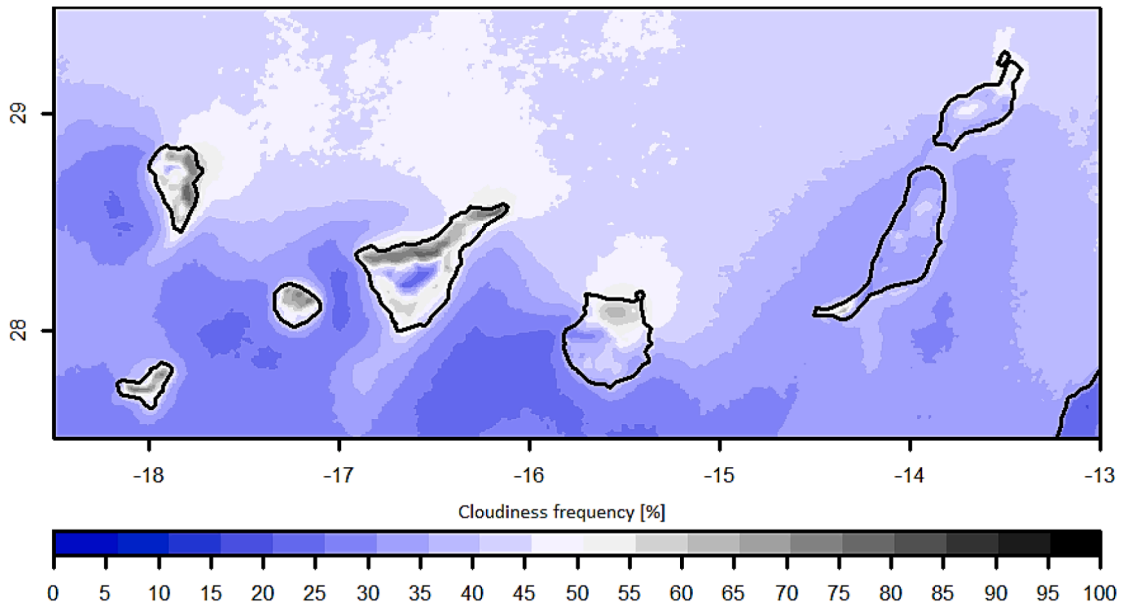

Fig. 5. Mean annual cloud frequency (%) at 400 m spatial resolution for the period 2000–2014.

micro-environments and it is in these places where the precision of the modelled climatic variables decreases and where observations tend to be scarce (Daly et al., 2002, Huade et al., 2005). In the Canary Islands, which are mountainous islands of volcanic origin, the multiple linear regression (MLR) methodology was chosen for the spatial modelling of climatological variables. MLR consists of obtaining a relationship between several independent or predictive variables (in this case related to topography) and a dependent variable (in this case related to climate). This interpolation method also allows testing of the suitability of multiple independent variables (Cohen et al., 2003). Therefore, parameters that influence precipitation (e.g. altitude, slope, orientation, etc.) can be used simultaneously. Such methods, involving multiple linear interpolation of climatic data combined with topographic data have been widely used in various parts of the world, improving map precision in areas of complex orography (Agnew and Palutikof, 2000; Ninyerola et al., 2000, Vicente-Serrano et al., 2003).

The MLR used as independent data the topographic information from a LiDAR-based 25 m spatial resolution digital terrain elevation map provided by Spain's National Geographic Institute (https://www.ign.es/web/ign/portal) and subsequently modified to 100 m resolution for use in the ACDIC atlas. The geographical parameters extracted from this digital map affecting the distribution of climatic variables were latitude (LAT), longitude (LON), elevation (ELE), orientation or aspect (ORI) and slope (SLO). Through linear regression of each of these geographical parameters and the homogenised data on the station points, a regression coefficient, a1,…,a5, shown in Eq.(2) below, was obtained for each time iteration (in this case 13 – to generate 12 monthly maps and one annual map). The result of the application of the spatial model, after determination of the regression coefficients, was not exact. To improve the map values, a residual layer (RES) was generated in parallel to represent the differences between the spatial model estimates and the input observations. The residuals represent the spatial variability not captured by the MLR model represented by Eq.(2). It is assumed that the errors of the model are independent and identically adjusted to a normal distribution with a mean of 0 and constant variance. These two assumptions are verified by applying the Durbin-Watson and Kolmogorov-Smirnov tests, as described in Marquínez et al. (2003). The inclusion of the residuals in the relationship significantly improves the fit results with respect to the observations (Agnew and Palutikof, 2000; Brown and Comrie, 2002). The residuals were spatially interpolated from the inverse of the weighted distance to generate a uniform layer over each island. The fitting process was carried out using the stepwise least squares procedure with forward variable selection (forward stepwise). The method allows all independent variables to be included in a single step and to discard in subsequent steps the variables that do not meet the expected statistical significance level ($p < 0.05$). The process is explained in detail in Marquínez et al. (2003) and Hession and Moore (2011). For the case of temperature, high significance was obtained with respect to latitude and elevation, concurring with the works of Ninyerola et al. (2000) and Daly (2006). The other climatological variables also showed dependence on slope and orientation, concurring with the works of Vicente-Serrano et al. (2003) and Nuñez Lopez et al. (2014) for the case of precipitation. In these works, the other independent variables which were studied, such as distance to the ocean as a measure of the effect of continentality, as well as earth sphericity and radiation necessary for large areas, were not considered in this work which focused on small islands surrounded by a large ocean.

Finally each point of the generated map (Y) at each time iteration depends on the obtained regression coefficients, the geographic parameters and the residuals, as shown below in Eq.(2):

$$Y = a_1 \bullet LAT + a_2 \bullet LON + a_3 \bullet ELE + a_4 \bullet ORI + a_5 \bullet SLO + RES \qquad (2)$$

In the final step of the interpolation, a maximum and minimum value limit was applied in areas with few observations (remote coastal areas, cliffs and high mountainous areas). Maximum and minimum thresholds were set on the basis of the homogenised climate series data to prevent the model from tending to unrealistic values due to remoteness from points with observations.

3.2.4. *Parameter specific steps*

Air temperature monthly series: A total of 420 meteorological stations distributed on the Canary Islands recorded minimum, maximum and mean air temperatures time series. Around 57 % were determined to be of use for this work due to the need to consider only those with a minimum length of 7 complete years in the period of analysis (1991–2020) as described in the filtering process. To fill data gaps in areas with few stations and to act as a guide for the others in the homogeneity adjustment, 39 ERA5-Land reanalysis points were incorporated. The reanalysis grid points required modification of their position with respect to their area of influence, but no farther than 2 km from their original position

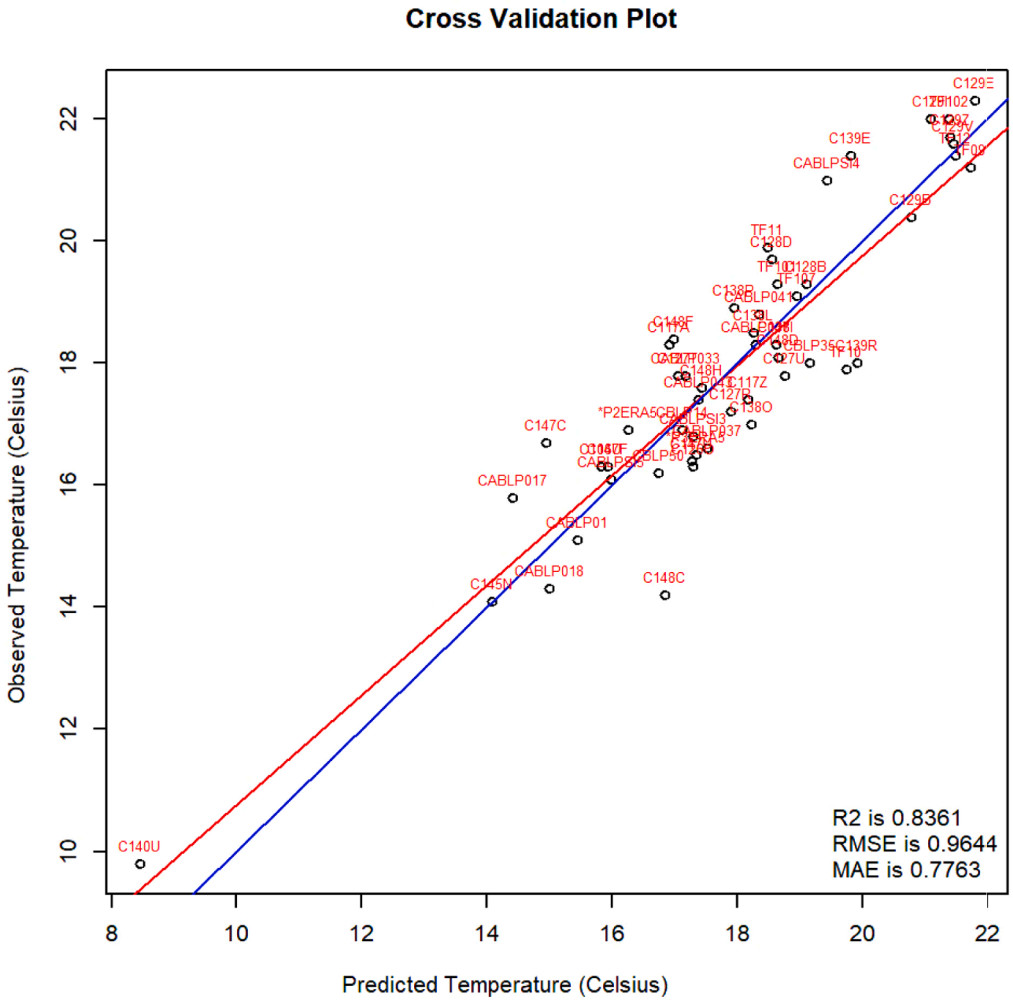

Fig. 6. Example of type of graph used as an evaluation tool after the generation of each map. Red codes are the station codes used in the verification. Here, the greater the number of points that are nearer to the blue diagonal line, the closer the R^2 value is to the optimal value of 1, and the lower are the error indices (RMSE and MAE).

and situated at the grid point reanalysis height on the 100 m spatial resolution map. Additional conditions to reduce evident anomalies in resulting climatic maps included new grid point locations being in zones influenced by the trade wind areas and the avoidance of gully bottoms. The second part of the filtering process comprised the detection of extreme temperatures in the series as proposed by Guttman et al. (1990). These were those which exceeded the threshold of three times the interquartile range above the third quartile (75 %) of the complete series (extreme high temperatures) and below the first quartile (25 %) of the series (extreme low temperatures). Prior to elimination of these extreme values, they were compared with those of the rest of the series to determine whether they might be related to heat waves or cold snaps. They were eliminated if these extreme values were found to occur in isolation without the appearance of extreme values in other series that coincided in time. In a third step, small gaps were filled by cross-correlation, comparing the series in the network by proximity. In general, for the whole archipelago 0.02 % of extreme values were eliminated, while 2.2 % of gaps were filled with respect to the total amount of data of the processed temperature series.

Monthly accumulated precipitation series: The precipitation series used to generate the maps were monthly accumulation in mm. Data processing in this case was similar to that for temperature, except that the reanalysis points were dispensed with. Of the 1,467 series available (Table 1), approximately 48 % could be used (706 series), with the removal of duplications in the series shared by AEMET and the Island Councils and of those that did not meet the general criterion of having at least 15 years of data in the analysis period in the filtering process. It should be noted that, given the irregularity of rainfall distribution in the Canary Islands in both time and space, the analysis period for precipitation map generation was increased to the maximum permitted by the availability of measurement series. It was found that this analysis period is not the same for all the islands. While in the province of Las Palmas (eastern islands) the period selected was 1970–2020, in the province of Santa Cruz de Tenerife (western islands) the period varied on each island due to the scarce number of series in the 1970s. Thus, the series for La Palma and El Hierro began in 1975, but for La Gomera in 1980.

Fig. 3 shows the average annual value of the series available for all islands. It can be seen that in the western islands (La Palma, Gomera, El Hierro and Tenerife) the largest number of operational series is concentrated in the period 1982–2008. As of this last year, the decrease in the number of series is drastic in El Hierro, where there are less than 10 series (there are months with only 5 data available for the entire island), and in La Gomera (where there are less than 15 rain gauges that record data). This was probably due to the impossibility of contracting meteorological observers or replacing them with automatic weather observation stations, as well as the absence of observation networks

Table 2
Description of the letter-based symbols of the climates found in the Canary archipelago based on the Köppen climate classification.

Initials	Climate type	Precipitation criterion	Temperature criterion
BWh	Hot desert	Scarce precipitation events, less than 200 mm annually	Mean annual temperature greater than 18 °C
BSh	Hot semi-arid	Scarce precipitation events, between 200 and 300 mm annually	Mean annual temperature greater than 18 °C
BSk	Cold semi-arid	Scarce precipitation events, between 200 and 300 mm annually	Mean annual temperature below 18 °C
Csa	Temperate climate with dry (s) and hot (a) summer	Precipitation below 30 mm in the driest summer month	Mean temperature of coolest month between 0 and 18 °C and temperature of warmest month 22 °C or above
Csb	Temperate climate with dry (s) and warm (b) summer	Precipitation below 30 mm in the driest summer month	Mean temperature of coolest month between 0 and 18 °C and temperature of warmest month below 22 °C
Dsc	Continental climate with dry (s) and cold (c) summer	Precipitation below 30 mm in the driest summer month	Mean temperature of coolest month below 0 °C and temperature of warmest month equal to or above 10 °C

other than those of AEMET, as is the case on the other islands. This problem was not observed in the eastern islands, where a wide network has been maintained through the work of numerous meteorological observers.

In the filtering process, in addition to discarding series of fewer than 15 years, the extreme values of each series were detected (considered as those that exceed the threshold of 9 times the standard deviation of the complete series). These were compared with the extreme values of the other series, and were eliminated if related to single isolated events and retained if extreme values were similarly found in temporally coincident series in their surroundings.

In the interpolation process, for the islands of higher altitude the stations were grouped as follows: N slopes with the influence of the trade winds from the first quadrant and S slopes, both below 1,200 m altitude, and the high zone above this altitude (shown by way of example for Tenerife in Fig. 8).

The final result comprises interpolated monthly cumulative rainfall maps (12 maps, one per month) and an annual cumulative rainfall map for each island. These monthly and annual accumulations were averaged for each island according to data availability. Thus, for the eastern islands with the largest amount of precipitation data the period was 1970–2020 and. with respect to the western islands, 1975–2020 for La Palma, El Hierro and Tenerife and 1980–2020 for La Gomera.

Relative humidity monthly series: The hygrometric information was taken from a total of 140 stations from AEMET, island Councils and SIAR (Table 1), distributed unevenly across the islands. Due to the scarce number of series in all the islands (except Tenerife thanks to the AGROCABILDO network: https://www.agrocabildo.org) it was decided to incorporate grid points with relative humidity data from the UERRA reanalysis (MESCAN-SURFEX) of 5.5 km spatial resolution, with the aim of completing the series in areas of low coverage by ground stations. This reanalysis was selected because it has a spatial resolution twice that of the ERA5-Land and is able to define in greater detail the relative humidity by altitude and on different slopes of the more mountainous islands. These reanalysis points were positioned in remote areas with a lack of measurement stations. Table 1 shows the number of stations per island and the institutions that provided the data series for generation of the mean monthly and annual climate maps of relative humidity for the period 1991–2020. However, on some smaller islands the period had to be shortened to 2018, when the UERRA reanalysis data concluded. In the filtering phase, in addition to eliminating short series, anomalous data with relative humidities below 20 % were detected and eliminated. In the interpolation phase, as in the case of precipitation, the islands of higher altitudes (La Palma, Tenerife and Gran Canaria) were separated into the same zones as for the case of the precipitation (see Fig. 9 for the case of Gran Canaria). The aim was to separate the summit zones, which have a significantly drier environment, above the layer of stratocumulus clouds (known locally as the "sea of clouds) whose limit in the Canary Islands is around 1,200 m above sea level (Dorta Antequera, 1996). Below this elevation, the N slope is cloudier and more humid than the S slope. Small mountainous islands such as La Gomera and El Hierro did not have enough stations to carry out this segmentation.

Wind speed monthly series: In this case, map development focused mainly on wind speed, not direction, due to the fact that in the Canary Islands, on average, N-NE trade winds predominate throughout the year. Winds in coastal waters and in the inter-island channels, areas with very few observations in general, are important. For this reason, reanalysis data were used to show this variable. The first analyses were performed with 10 km resolution ERA5-Land and 5 km resolution UERRA (MESCAN-SURFEX) surface data from the last 20 years (2001–2020). These revealed that higher spatial resolution data, such as UERRA, are able to represent in greater detail wind speeds in offshore areas, especially in the inter-island channels, which are affected by higher wind speeds. Fig. 4 shows the annual mean (a), July mean (b) and January mean (c) for the last 20 years at 400 m spatial resolution.

Subsequently, wind speed maps at 100 m spatial resolution of the land surfaces of each island were obtained from the data of the observation stations and the inclusion of surface UERRA data (UERRA MESCAN-SURFEX) in coastal points and areas with few observations on slopes. UERRA-HARMONIE – points were added in high altitude areas with few observations. However, these are not surface data but based on pressure level layers. These reanalysis data were also obtained from the Copernicus website and are represented in Table 1. The large number of UERRA MESCAN-SURFEX surface points stands out in this table, as they

Table 3
Statistical results comparison of map-obtained, minimum (Min), mean (Mea) and maximum (Max) annual air temperatures (degree Celsius) with the observed annual mean for the 1991–2020 period.

Islands	Definitive no. of stations	R2 (squared correlation)			RMSE (root mean squared error)			MAE (mean absolute error)		
		Min	Mea	Max	Min	Mea	Max	Min	Mea	Max
La Palma	45	0.83	0.90	0.88	1.11	0.84	0.89	0.85	0.60	0.68
La Gomera	25	0.86	0.89	0.85	1.13	0.89	0.99	0.98	0.72	0.83
El Hierro	20	0.90	0.90	0.84	0.95	0.88	1.08	0.78	0.68	0.87
Tenerife	115	0.81	0.86	0.83	1.30	0.94	1.03	0.95	0.74	0.82
Gran Canaria	44	0.78	0.86	0.70	1.21	0.82	1.13	1.01	0.67	0.96
Fuerteventura	13	0.37	0.27	0.26	1.20	0.82	1.10	0.56	0.68	0.80
Lanzarote	21	0.54	0.60	0.62	0.69	0.61	0.58	0.58	0.47	0.46

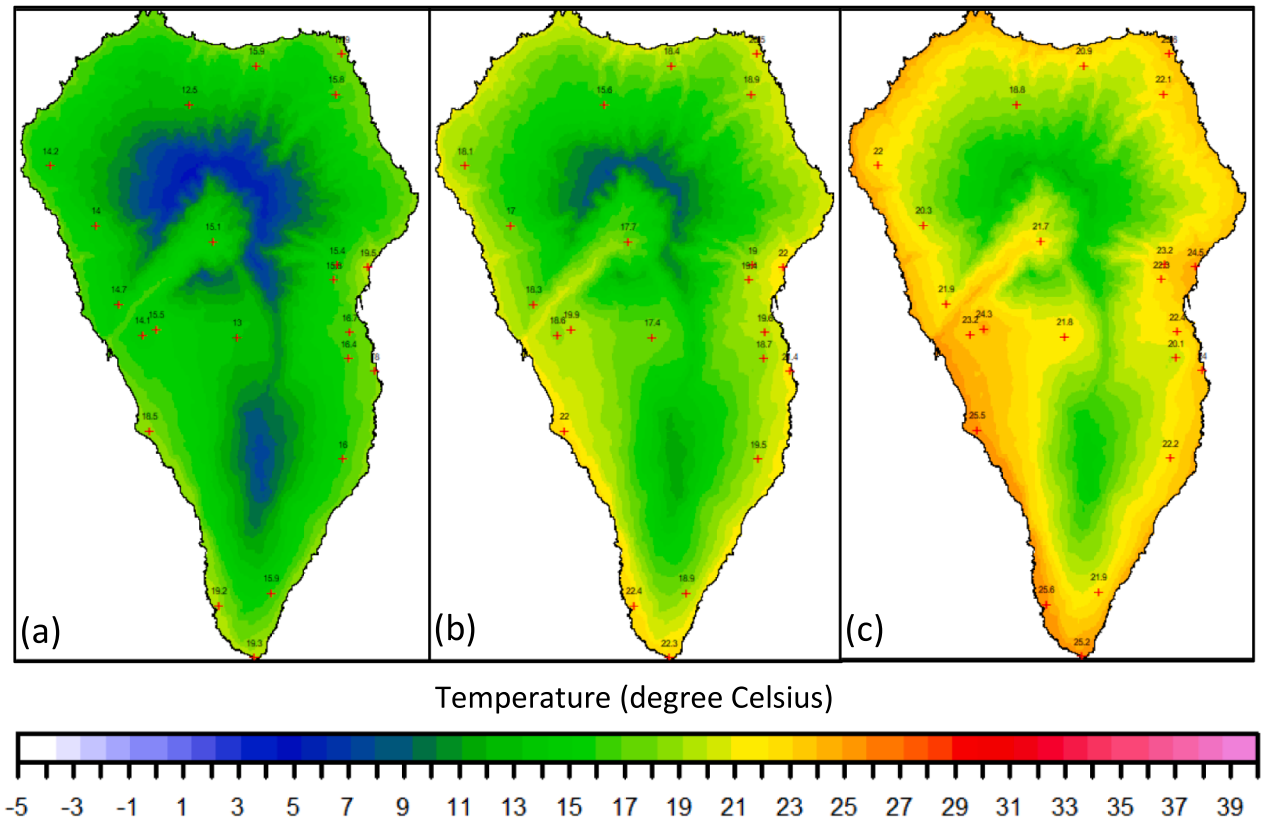

Fig. 7. Air temperature maps of La Palma Island at 100 m resolution averaged for the 1991–2020 period. (a) Minimum temperature, (b) Mean temperature, and (c) Maximum temperature. Crosses indicate the position of the meteorological stations used and the values are the means from observed air temperatures.

are points over unobstructed coastal waters that surround each island.

Finally, the multiple linear regression interpolation process was applied to each island, separating those with the highest altitudes into eastern and western zones and altitudes below and above the stratocumulus cloud layer in the inversion level in 1,200 m.

Cloudiness: The determination of cloudiness was based on remote sensing data from the MODIS (Moderate Resolution Imaging Spectroradiometer) sensor of 1 km resolution. The determination of mean monthly and annual cloud frequency for the period 2000–2014 was performed following the methodology and data provided by Wilson and Jetz (2016). The procedure involved calculating the monthly cloud frequency at each point from the 4 daily MODIS sensor images obtained by NASA's two polar-orbiting satellites (Terra and Aqua). However, as described, the two day-time images and related cloudiness products were used to avoid a decrease in accuracy when using only infrared channels in the determination of cloudiness with the two daily night-time images. More specifically, the MOD09GA cloud flag derived from the Terra satellite was used, which passes over each day at about 10:30 local time, and the MYD09GA from the Aqua satellite, which passes over at about 13:30 local time. These products, as described by Liu and Liu (2013) for the latest versions, use various cloud classification algorithms to appropriately separate cloudy areas from land surfaces. In particular, there is improved differentiation of those with high albedo such as water with specular reflections, or snowy, sandy and urban regions. These files (MOD09GA and MYD09GA) were compiled between February 2000 and March 2014 and provide a positive (cloudy) or negative (non-cloudy) value for each point and each day. Therefore, the monthly and annual proportion of cloudiness in each kilometre of the globe was calculated and stored in *GeoTIFF* files that are freely available (http://www.earthenv.org//cloud). For the interactive atlas, these monthly and annual files were downloaded and a climatology of the cloudiness of the Canary archipelago was obtained. The mean annual cloudiness frequency for the period 2000–2014 is shown at about 400 m spatial resolution in Fig. 5.

After carrying out these processes with the monthly data series, month- and year-based maps were obtained for each averaged variable for the period analysed. Data periods are shown in Table 1. It should be noted that these periods may differ to some extent for each island depending on data availability. The final step, after a review of the results, was to make them available to the user through a web tool developed for this purpose.

Table 4
Statistical results comparison of map-obtained annual cumulative precipitation in mm with the observed values for periods ranging from 1970, 1975 or 1980 to 2020, depending on the island.

Islands	Definitive no. of stations	Analysis period	R2 (squared correlation)	RMSE (root mean squared error)	MAE (mean absolute error)
La Palma	48	1975–2020	0.99	20.5	14.34
La Gomera	26	1980–2020	0.85	65.6	56.2
El Hierro	26	1975–2020	0.50	104.3	82.1
Tenerife	141	1975–2020	0.98	22.7	14.8
Gran Canaria	344	1970–2020	0.91	51.2	40
Fuerteventura	56	1970–2020	0.77	14.8	12.3
Lanzarote	65	1970–2020	0.82	11.9	9.1

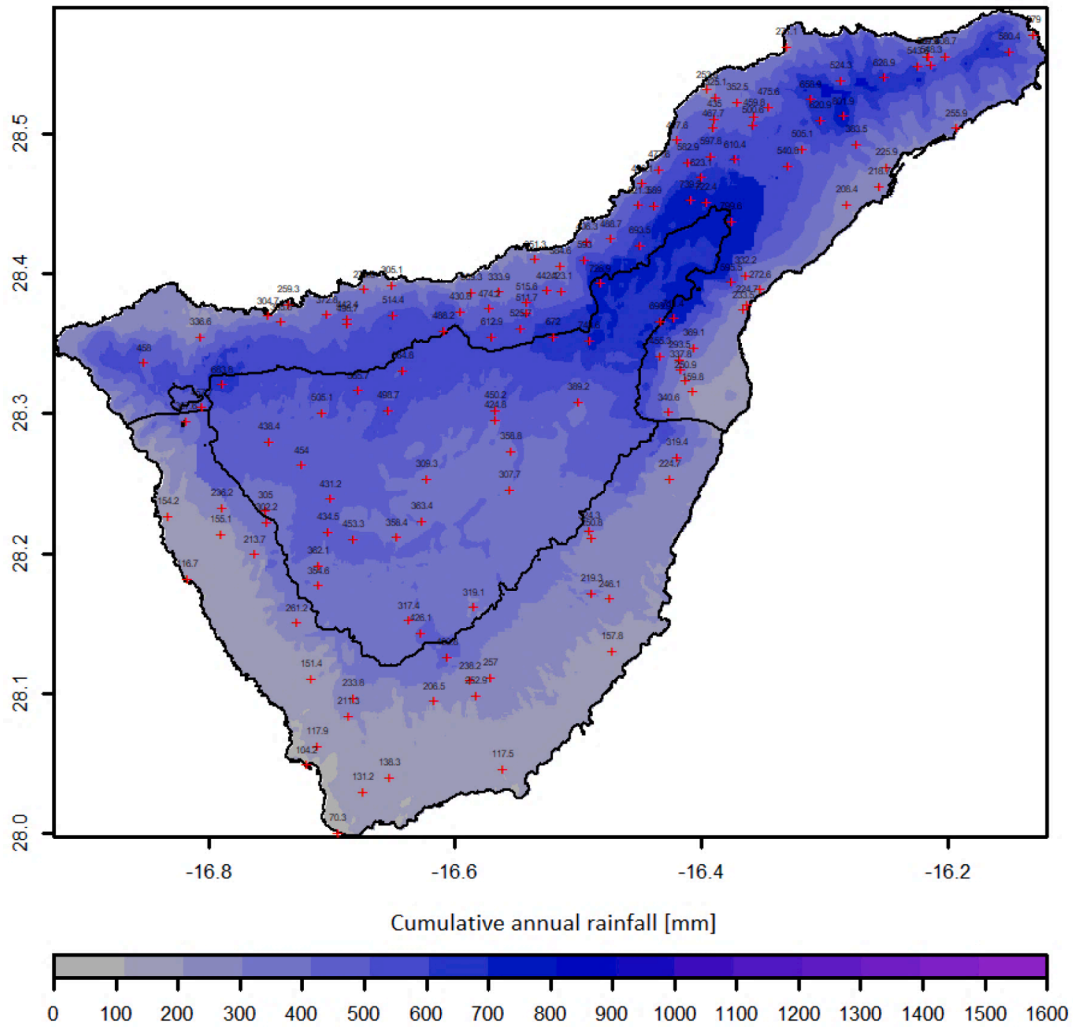

Fig. 8. Cumulative annual rainfall in mm at 100 m resolution for Tenerife and the period 1975–2020. Crosses indicate the position of the meteorological stations used and mean annual accumulations from the observations. Also shown, separated by black lines, are the northern, southern and high altitude (over 1,200 m) areas.

3.2.5. *Maps evaluation*

For purposes of evaluation, after the generation of each map a graph was generated showing on its horizontal axis the result predicted by the regression model and on its vertical axis the homogenised observed data, as shown in the example in Fig. 6. The best result is one in which the points of each station (identified by its code) lie on the ideal diagonal line (represented in blue). After the 'true' linear fit (represented in red), three statistics were obtained: the squared correlation coefficient (R^2), the root mean squared error (RMSE) and the mean absolute error (MAE). It should be noted that the result predicted by the regression model in the evaluation graph does not consider the observed point in model coefficient and adjustment fit, doing a pure model prediction comparison with respect to observation in each location point. Therefore, the evaluation is representative of the model mainly in areas without observations. These graphs were used to identify stations with outlier results far from the diagonal and therefore subject to individual revision by returning to the filtering process for their elimination or to the homogenisation process for their subsequent correction.

3.2.6. *Köppen climate classification maps*

Initially conceived by the German physicist Wladimir Köppen in 1918, and subsequently revised by himself and Rudolf Geiger in 1936, the Köppen classification defines different types of climate on the basis of monthly mean values of precipitation and air temperature. For the delimitation of different climate types, temperature and precipitation thresholds are established based principally on their influence on the distribution of vegetation and human activity, with the world's climates divided into five main groups: tropical, arid, temperate, continental and polar, identified by the capital letters A, B, C, D and E, respectively. Each group is further divided into subgroups describing a climate type, indicating temperature and precipitation behaviour. Climate types are thus identified by a 2 or 3 letter symbol.

The Köppen climate classification maps obtained for the Canary archipelago from the monthly and annual maps of minimum, maximum and mean temperature, in addition to the precipitation maps for the last 30 years (1991–2020). Monthly and annual temperature and precipitation maps were obtained from the ACDIC as explained previously. Table 2 gives a detailed description of the main climate types with their acronyms and the Köppen climate temperature and precipitation thresholds used to develop the classification maps.

3.2.7. *Trend maps*

Analyses of mean temperature and precipitation trends are of great importance to assess the changes in the islands climate, as they allow us to diagnose alterations in the studied variables over the last 30, 40 or 50 years resulting from anthropic actions.

Given a time series (e.g. temperature), the trend is the rate at which this variable changes over a period of time. The trend can be linear or non-linear. Simple linear regression is commonly used to estimate the linear trend (slope) and the statistical significance (using a Student's *t*-

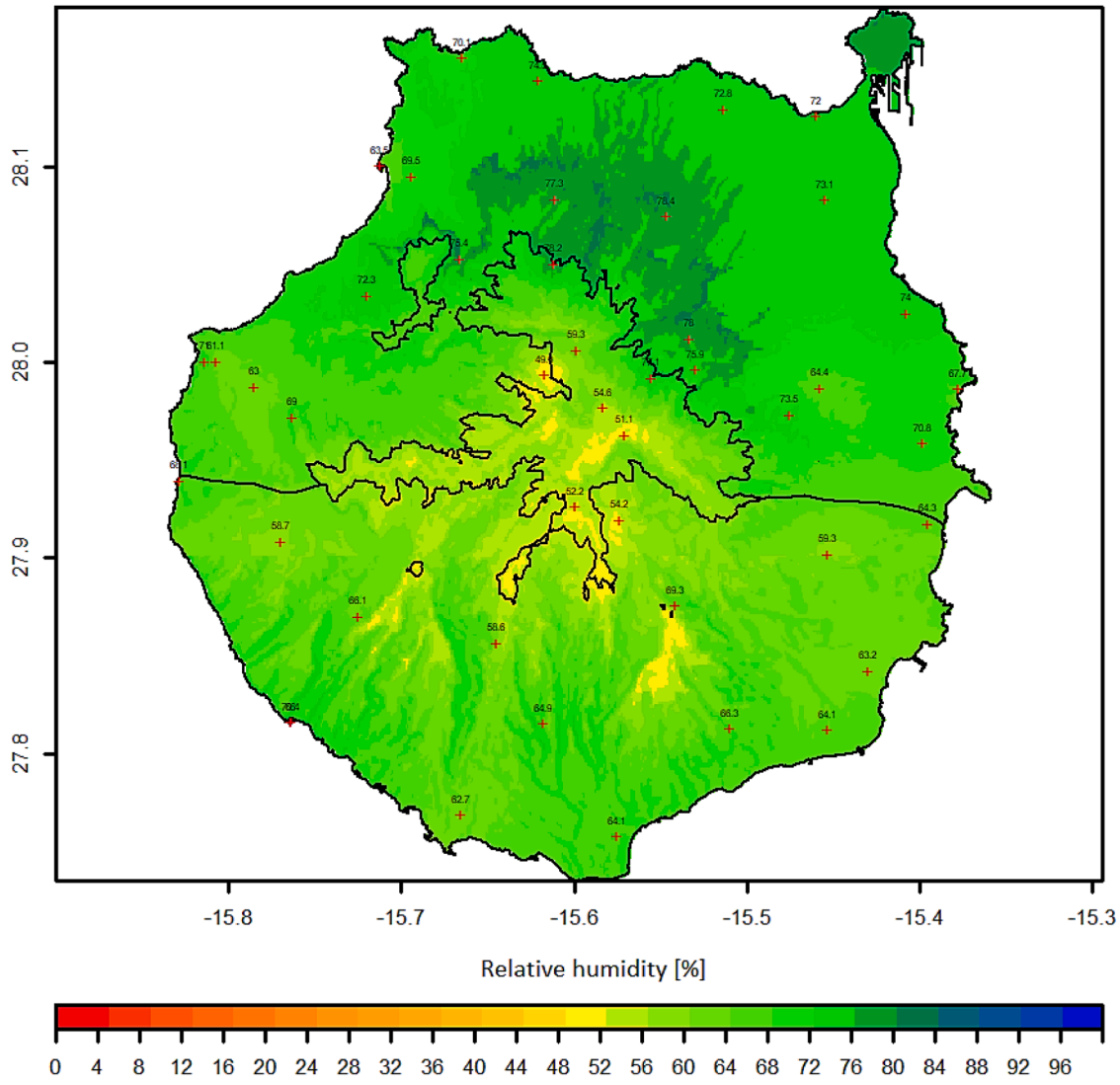

Fig. 9. Mean relative humidity (%) at 100 m resolution for Gran Canaria and the period 1991–2020. Crosses indicate the positions of the weather stations used and the values are the means from observed relative humidities. Also shown, separated by black lines, are the northern, southern and high altitude (over 1,200 m) areas.

Table 5
Statistical results comparison of map-obtained mean annual relative humidity (in %) compared with weather station observations (1991 to 2018 or 2020).

Islands	Definitive no. of stations	Analysis period	R2 (squared correlation)	RMSE (root mean squared error)	MAE (mean absolute error)
La Palma	43	1991–2018	0.98	1.20	0.84
La Gomera	13	1991–2018	0.68	3.08	2.16
El Hierro	11	1991–2018	0.52	4.66	4.01
Tenerife	71	1991–2020	0.98	1.07	0.71
Gran Canaria	44	1991–2020	0.96	1.68	1.17
Fuerteventura	26	1991–2018	0.65	2.83	2.33
Lanzarote	20	1991–2018	0.55	2.43	1.99

test). However, in this work we used a procedure based on the Mann-Kendall test and the method developed by Theil (1950) and Sen (1968). The non-parametric Mann-Kendall test (Kendall, 1975, Mann, 1945) was applied to determine the series with linear trends in annual temperatures and precipitations. This test has two fundamental advantages: i) as it is a non-parametric test it does not require series with normal distribution; and ii) it is not so sensitive to the lack of data. The test establishes that the null hypothesis is that there is no linear trend in the series, meaning the data are independent and randomly distributed. The alternative hypothesis is that there is a linear trend in the time series. The statistical significance threshold can be established considering different probability levels (p values) of the Z variable of the test. These thresholds can be established according to the characteristics of the precipitation: very low in some cases, with $p < 0.7$ which is equivalent to 30 % statistical significance (Máyer et al., 2017); higher in other cases, with $p < 0.10$ which corresponds to a level of significance of 90 % and $Z = 1.645$ (Cortesi et al., 2012); or in cases that require greater precision, with $p < 0.05$ or $p < 0.01$ which correspond to 95 % and 99 % statistical significance, respectively (Cropper and Hanna, 2013). In this work, a level of significance of 90 % was taken due to the unpredictable character of precipitation in the islands. The trends were calculated using the method of Theil (1950) and Sen (1968), which applies a linear

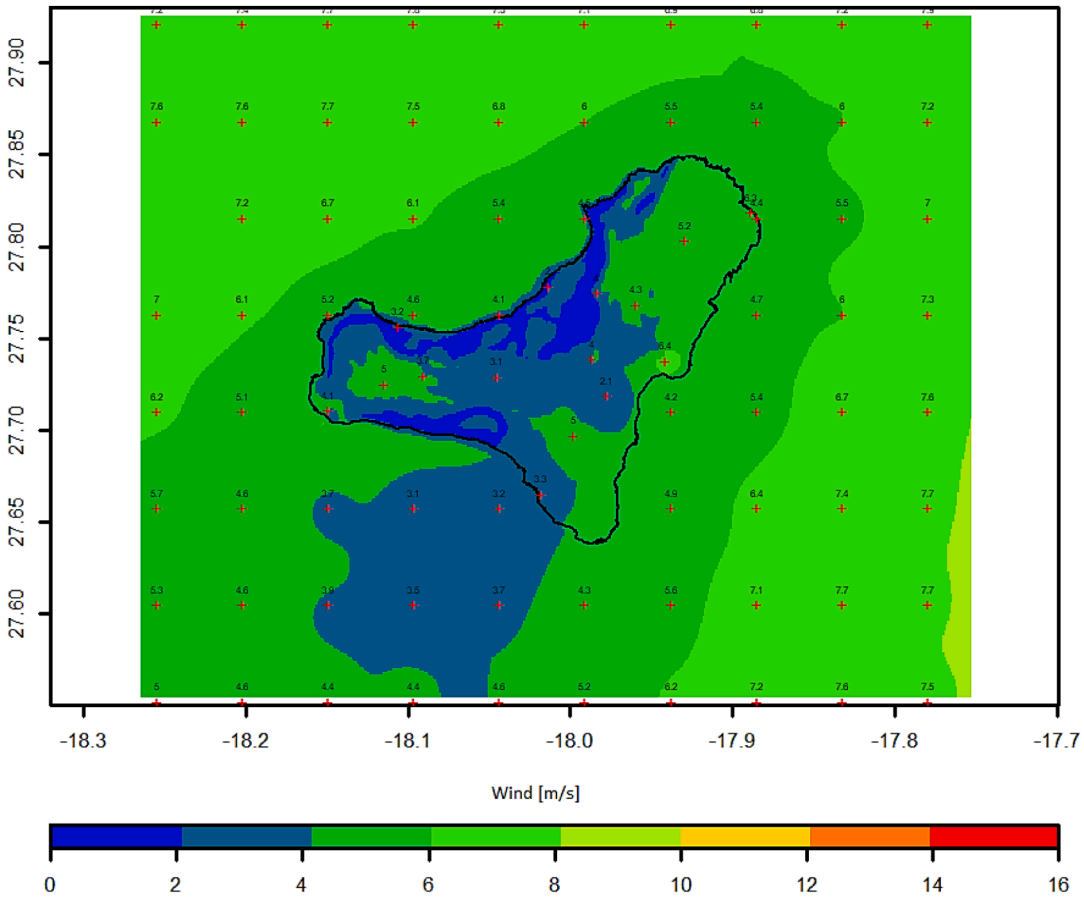

Fig. 10. Annual mean wind speed map in m/s for the period 2001–2020 corresponding to the island of El Hierro.

regression model for cases of monotonic trend. It is a non-parametric method, with some advantages such as robustness in the case of outliers, and does not assume a specific shape of the time series, unlike others which suppose a strictly linear shape. A semi-transparent mask was superimposed on the trend maps obtained for those points with p-values of the Mann-Kendall S-statistic above 10 % ($p > 0.1$) and, therefore, of lower statistical significance than 90 %.

4. Results

The results are shown below, indicating the data used, the problems detected in each variable and examples of some of the maps obtained. The different variables are temperature (minimum, mean, maximum), precipitation, relative humidity, wind speed, and cloudiness. Also included in this section are the Köppen climate classification maps and the decadal trends of temperature and precipitation.

4.1. Air temperature

Table 3 shows the statistical results after generation of the minimum (Min), mean (Mea), and maximum (Max) temperature maps for all the islands, comparing the annual average of the modelled map points with the observed annual average for the 1991–2020 period. In general, squared correlations of around 0.80 and errors of between 0.60 and 1 °C were observed, except for Lanzarote and Fuerteventura which had lower squared correlations of between 0.30 and 0.60. Fig. 7 shows, by way of example, the minimum, mean and maximum temperature maps for the island of La Palma at 100 m resolution.

4.2. Precipitation

For precipitation, Table 4 compares the annual accumulation of the points of the modelled maps with the annual accumulation observed for the period analysed on each island. It can be seen that El Hierro and La Gomera have the largest errors, presumably due to the low number of stations with long series of more than 15 years. Fig. 8 shows the cumulative annual rainfall for Tenerife in the northern, southern and high altitude (above 1200 m) areas. Note that on this island the greatest amounts of precipitation, between 600 and 800 mm, are found around the 1200 m isoline indicated on the map which separates the northern area and the high altitude area.

4.3. Relative humidity

Table 5 shows the statistical results when comparing the mean annual relative humidity over the 28–30 year period obtained from the maps with the observed values on each island. Again, it is clear that the statistical results with the highest error were for small islands such as La Gomera and El Hierro with few measuring stations and islands of low altitude such as Lanzarote and Fuerteventura. Fig. 9 shows, by way of example, the mean annual relative humidity for Gran Canaria and the period 1991–2020. The highest values correspond to the cloud zone between 700 and 1,200 m above sea level on the N and NE slopes, while the areas with the lowest relative humidity are located over 1,200 m above sea level, and on the S and SW slopes of the island.

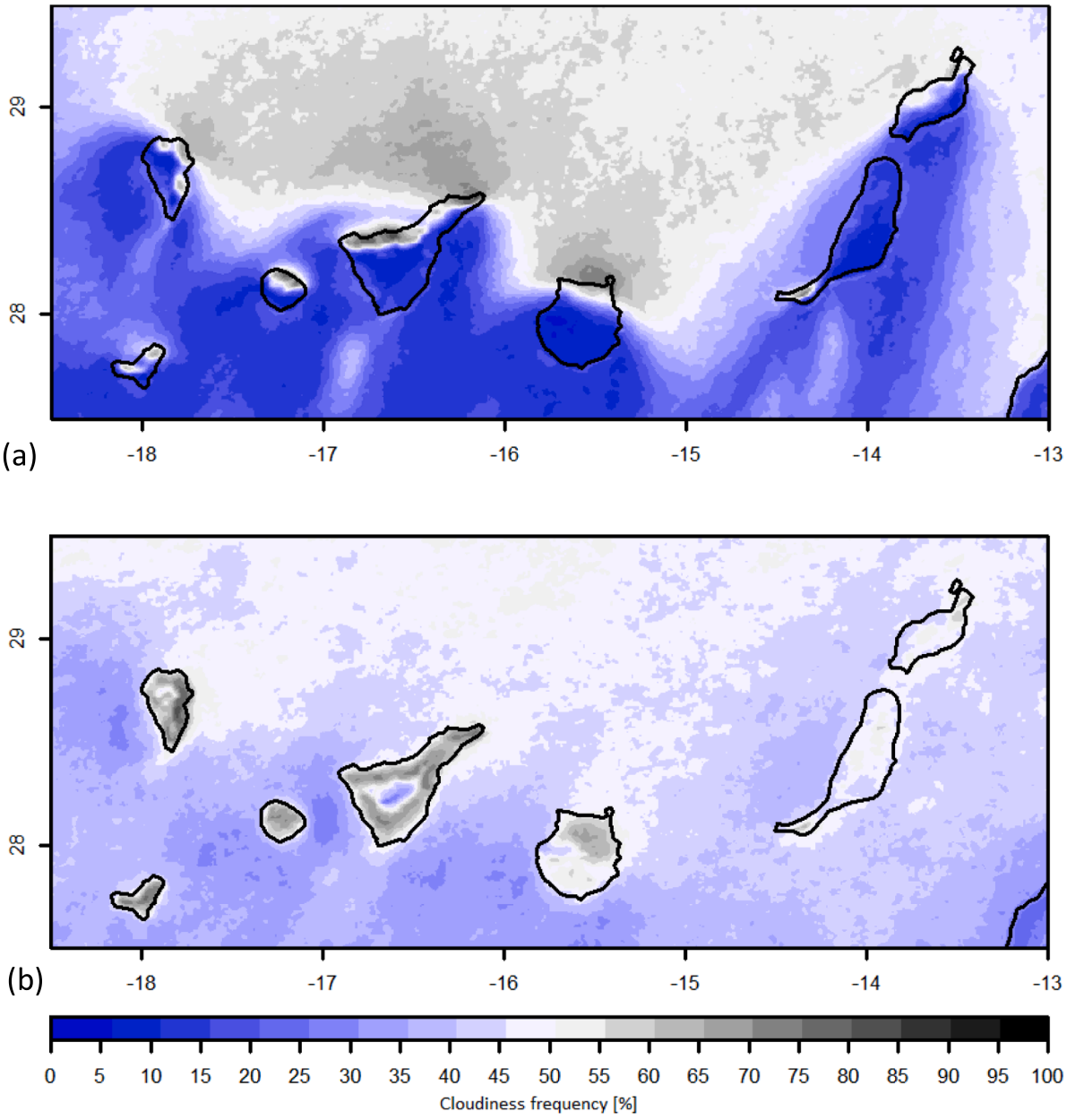

Fig. 11. Monthly cloudiness frequency (%) in July (a) and January (b) at 400 m resolution and averaged for the period 2000–2014.

Table 6
Percentage of area affected by each climate type in each island.

	Area* (Km^2)	BWh (%)	BSh (%)	BSk (%)	Csa (%)	Csb (%)	Dsc (%)
La Palma	708.32	4.0	11.8	0.6	12.2	71.5	0.0
El Hierro	268.71	10.0	33.5	6.4	13.9	36.1	0.0
La Gomera	369.76	13.8	32.2	3.7	12.1	38.3	0.0
Tenerife	2,034.38	15.6	17.6	5.8	12.7	48.0	0.4
Gran Canaria	1,560.10	36.0	30.0	5.4	18.8	9.8	0.0
Fuerteventura	1,659.74	93.8	1.1	5.0	0.0	0.0	0.0
Lanzarote	845.94	95.5	2.4	2.1	0.0	0.0	0.0

* Canarian Institute of Statistics (ISTAC: https://www.gobiernodecanarias.org/istac/).

4.4. Wind speed

The statistical comparison of map-obtained mean wind speed for the 2001–2020 period compared to observed values gave an R2 of 0.79, an RMSE of 0.48 m/s and an MAE of 0.41 m/s. Fig. 10 shows the wind speed map for the island of El Hierro. Note the blocking of the trade winds by the relief both to the N and SW and the increase in intensity in the NE waters and coasts. It should also be noted that this trade wind blocking is not as significant on low lying islands such as Lanzarote and Fuerteventura. In high summit areas, above the stratocumulus layer, the intensity of the frequent NE winds is less notable, on average, compared to lower areas.

4.5. Cloudiness

Although originally the data were at 1 km resolution, they were reprojected at 400 m resolution by smoothing and colouring every 5 %. This figure shows bluish areas to the SW and summits of the most mountainous islands with a lower annual frequency of cloudiness, of around 30 %, while at the other extreme greyish tones highlight the cloudiest areas to the N and NE of the most mountainous islands with

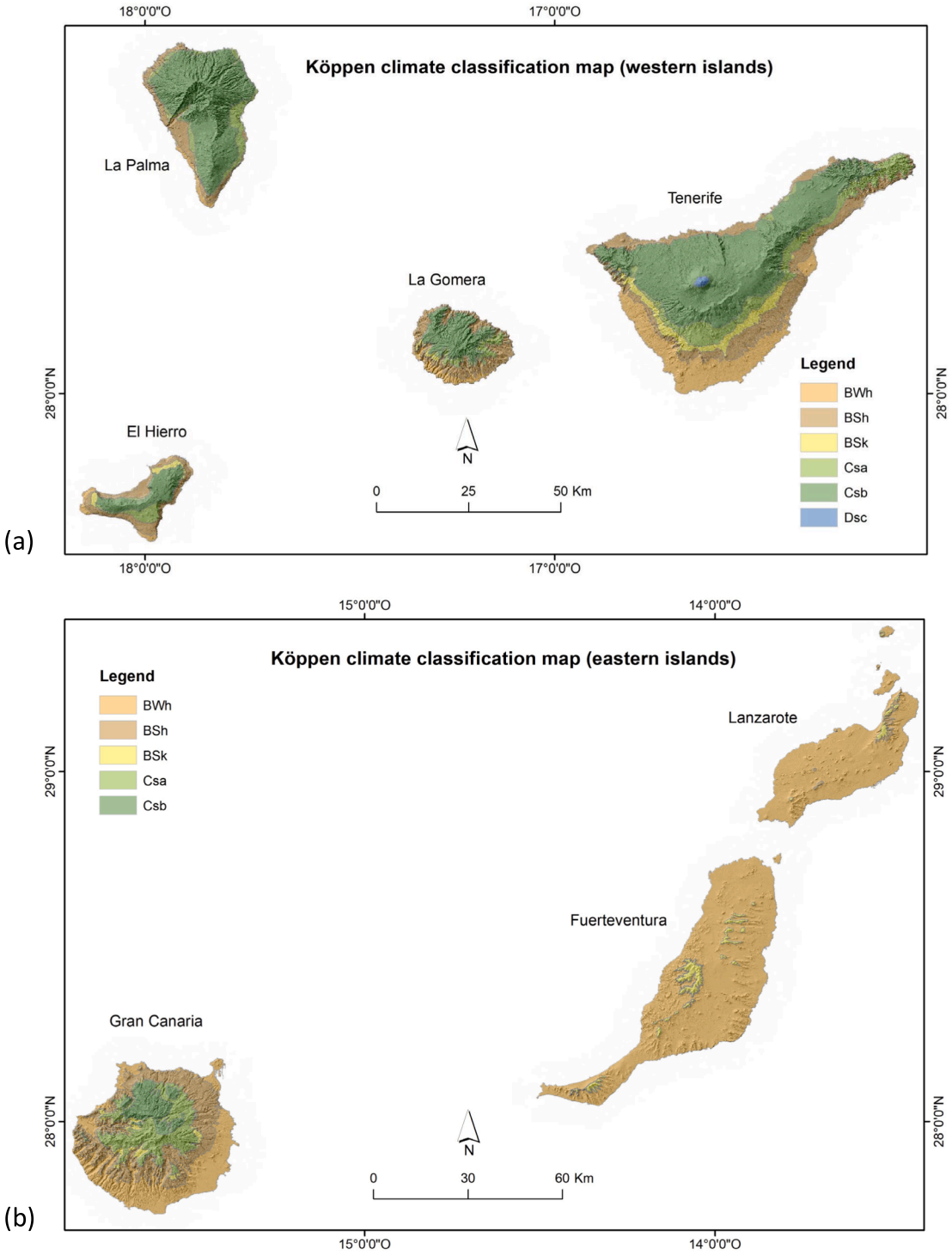

Fig. 12. Köppen climate classification maps at 100 m spatial resolution obtained from the ACDIC data in the recent period from 1991 to 2020 (a) western islands, (b) eastern islands.

frequencies above 60 %. Fig. 11 shows the cloudiness frequency in July (a), dominated by the cloudiness associated with the trade winds which mainly affects the coastal areas and midaltitude areas and facing N and NE, and in January (b) with a higher frequency of cloudiness at higher altitudes caused by different meteorological situations in addition to the trade winds.

4.6. Köppen climate classification maps

According to previous works (López Gómez and López, 1979; Morales and Pérez-González, 2000), two main climate types can be considered in the Canary Islands: arid climates (B), in which annual rainfall is lower than annual potential evapotranspiration, and temperate climates (C), whose main characteristic is humidity and temperatures that oscillate between different ranges (mean temperature of the coldest month between 3 °C –or 0 °C- and 18 °C and mean

Table 7
Period of study (by start and end year, mainly from 1991 to 2020). Sites by island with decadal temperature trends statistically greater than 90% in °C/decade units.

Island	Trend start year	Trend end year	Total no. of years	Cooling or minimum trend recorded and zone (°C/decade)	Warming or maximum trend recorded and zone (°C/decade)
La Palma	1991	2020	30	Not observed	+1.4 for the NE and + 0.4 for the E and W coasts
La Gomera	1991	2020	30	Not observed	+1.2 for the peak and + 0.8 for the E
El Hierro	1991	2020	30	Not observed	+0.8 for the W and N
Tenerife	1991	2020	30	−0.8 for Buena Vista-Teno (NW), −0.6 for Benijos-Agua Mansa (N centre)	+0.8 for the triangular area Adeje-Vilaflor-Granadilla, +0.2 to + 0.8 for the E coast from El Médano to San Andrés
Gran Canaria	1991	2020	30	−0.4 for Agaete gorge (NW)	+0.8 to + 1.4 for the triangular area Mogán-Fataga-Maspalomas, +0.4 to 0.8 for the SW coast
Fuerteventura	1991	2020	30	Not observed	+0.4 for Morrojable and the SE coast and the SE inland area from Gran Tarajal to the airport
Lanzarote	1993	2020	28	Not observed	+0.2 to + 0.4 for Playa de Famara and the E coast from Puerto del Carmen to Arrieta

temperature of the warmest month above 10 °C).

From the Köppen climate classification maps obtained in this study using the recent data, the two main climate types were B and C, as expected. A small area was also identified with climate type D (continental) with very cold winters and cool summers in the higher areas of Teide in Tenerife. Table 6 shows the percentage of area affected on each island by each climate type. The Fig. 12 shows the Köppen climate maps obtained with the ACDIC data from 1991 to 2020.

4.7. Trend maps

The total time period of monthly and annual mean temperature trends was established from 1991 to 2020 with an annual frequency for all the islands, as can be seen in Table 7. The monthly and annual rainfall trend, however, is from 1970 to 2020, some 50 years, except for the western islands where the first year had to be later due to data scarcity for certain slopes in the 1970 s and early 1980 s. Thus, for La Gomera the first year of the precipitation trend map is 1980, for El Hierro it is 1985 and for La Palma and Tenerife it is 1986. For the same reason of data scarcity, the calculation of temperature trends for the island of Lanzarote begins in 1993.

The temperature unit of measurement is change in degrees Celsius (°C) per decade. Table 7 shows the periods in years used for each island, as well as the general results of maximum (warming) and minimum (cooling) decadal trends, based on the annual averages of the mean temperature maps. Fig. 13 shows the mean decadal temperature trend maps for the Canary Islands, with warming indicated in reddish-orange and cooling in bluish-grey. A semi-transparent mask formed by small black squares shows areas with statistical significance trends lower than 90 %.

The equivalent for the decadal trends of monthly precipitation can be seen in Table 8, while the decadal trend of precipitation for the islands is presented by way of example in Fig. 14. Areas with a decreasing precipitation trend are shown in brown-orange and those with an increasing precipitation trend in grey-blue. In general, areas with low statistical significance predominate the precipitation maps on all islands, except the island of Fuerteventura where most of the area shows a mean annual precipitation trend of −2 mm/Decade. In this figure the most populated islands are zoomed, and colours are a bit intensified with respect the web facility to let a better identification of areas.

5. Discussion

For the first time in the Canary Islands, a project is being undertaken with the aim of providing society with a set of useful climatic resources for multiple areas, from regional and local administrations (planning and management of the territory, education, environment, etc.) to professionals and citizens in general who demand climate information. As explained in the Introduction section, while this type of initiative has been carried out in various countries and regions in no other case have the trends of precipitation and air temperature been incorporated, something we consider of interest and importance in a context of global warming.

Regarding the initial data, a significant effort was made to compile the available data from multiple databases managed by different public administrations. However, as not all the variables have good spatial or temporal coverage other data sources were also used. From a methodological point of view, the work has some novel aspects including the combination of observational networks from different administrations and the integration of reanalysis points in climatic databases. This second process was carried out only in those cases where the observations were insufficient to characterize a variable. In addition, the procedure used in the generation of maps with the highest spatial resolution and precision which the initial data can admit involved the application of a multiple linear regression model. This method has been widely used in regions of complex topography, as evidenced by the works of Agnew and Palutikof (2000), Ninyerola et al. (2000) and Vicente-Serrano et al. (2003), among others. This procedure for generating climatological maps was considered ideal for this case of mountainous Atlantic islands of volcanic origin, and is similar to the procedure employed for the atlas of the Canary Islands, Madeira and the Azores developed by the national weather centres of Spain and Portugal (AEMET, 2012).

With regard to the results, it should be noted that they are consistent with some previous studies in the Canary Islands including, for example, the climatic atlas of the Macaronesia islands (AEMET, 2012). With a methodology similar to this work for air temperature, a multiple linear regression was employed for the Macaronesia atlas with altitude, latitude and longitude as auxiliary variables, interpolation of the residual component using the inverse of the weighted distance, a resolution of 100 m and a time period covering the years 1971–2000. The maps of average air temperature and annual precipitation are similar to those of this work. In the case of the first variable, differences can be detected in the high altitude areas above the inversion level (1,200 m) of around 1.0 °C − 2.0 °C in the case of the peaks of Tenerife, Gran Canaria and La Palma, probably due to the fact that the work presented here is based on the generally warmer recent period of 1991–2020. This is in line with the analysis carried out in this work on the trends of this variable, as will be discussed later. In the case of precipitation, the values are similar in both works, with the areas of greatest accumulation coinciding with the slopes located between 700–900 m in the northeast of the island of La Palma (1,200 and 1,400 mm), the north of Tenerife and Gran Canaria and the peaks of La Gomera and El Hierro (between 700 and 800 mm). Only in the case of the island of Tenerife do the accumulated annual precipitation values reach 900 mm (Aemet, 2012) for the previous period between 1970 and 2000.

The AEMET atlas (2012) displays Köppen climate classification maps obtained for the period 1971–2000. When comparing these with those obtained in the present study, representative of a more recent period (1991–2020), a notable similarity can generally be observed in the classified areas except for some small details. For example, on Tenerife, the highest island and with the greatest climatic diversity, in the AEMET (2012) Köppen climate classification map, the Csa climate (temperate

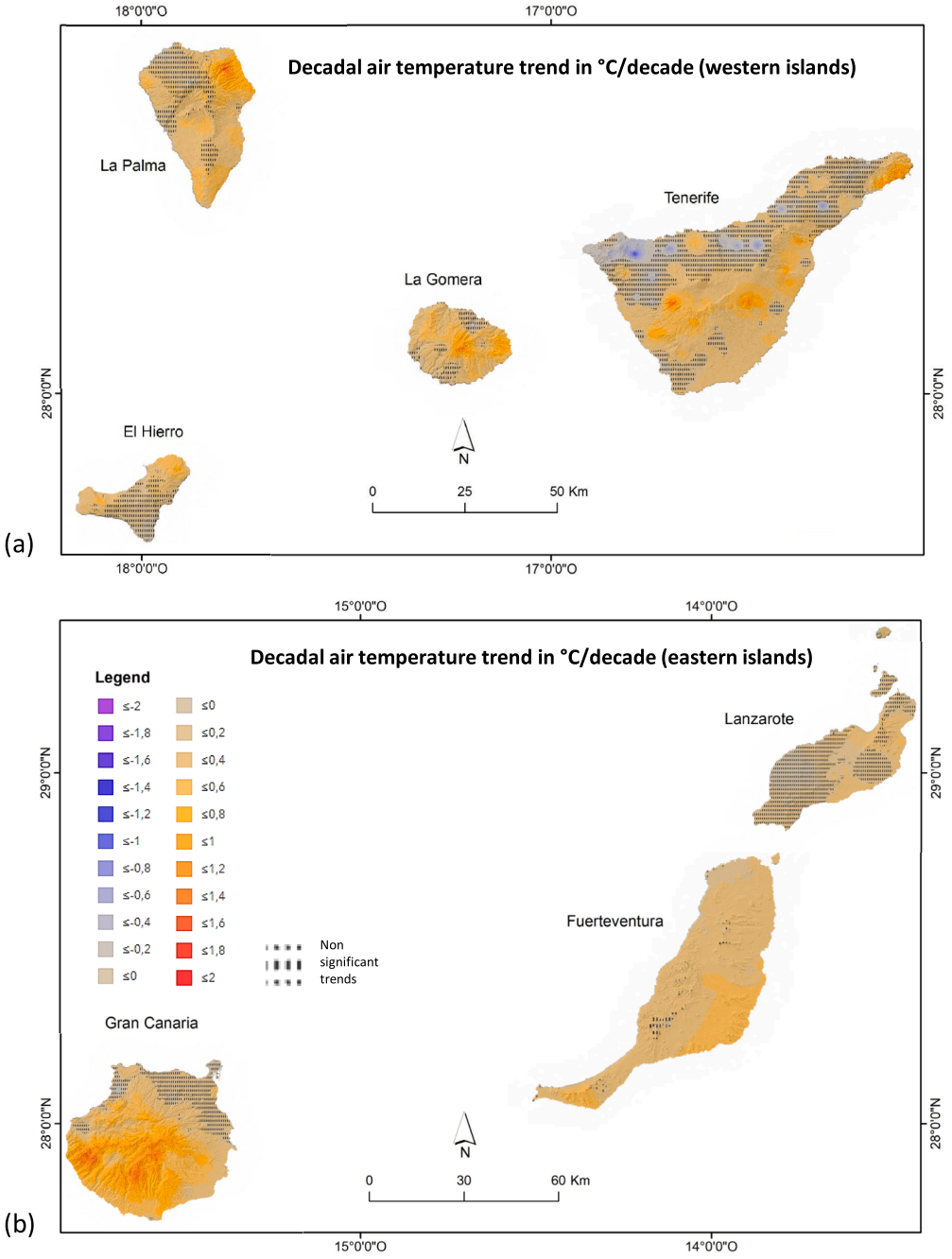

Fig. 13. Decadal temperature trend in °C/decade between 1991 and 2020 for the Canary Islands in a 100 m spatial resolution map (a) western islands, (b) eastern islands.

with dry and hot summers) is barely observed. However, in the results for the period 1991–2020 obtained in the current work, the Csa climate represents 12.7 % of Tenerife (Table 6). This peculiarity of the appearance of hot summers in temperate zones that previously had warm summers is also observed in small islands such as La Gomera and El Hierro. Therefore, it is, presumably, a sign of recent warming that is affecting summers in these temperate zones.

The trend areas with statistical significance above 90 % based on the Mann-Kendall test (Table 7) were extracted from the air temperature trend maps (Fig. 13) obtained for the Canary Islands in this study. In this table, a general trend towards warming rather than cooling can be discerned in the period analysed (1991–2020). Most notable is the warming observed on Gran Canaria, especially in the southwest and summit areas. Although the warming varies by island and area, as can be observed in the maps, an average of 0.33 °C/decade was obtained for Tenerife and an even more pronounced average warming of 0.45 °C/decade for Gran Canaria. In previous studies, Martín et al. (2012) and Luque et al. (2013) obtained trends on these islands of 0.09 °C/decade in the long period between 1944 and 2010, increasing to 0.17 °C/decade if the period is shortened to 1970–2010. Given these results from previous studies and the trends obtained in the ACDIC maps for the 1991–2020 period, it can plausibly be argued that warming is increasing at an accelerated rate on these islands.

The precipitation trend maps obtained in this study for the recent period of 1980–2020 show a large proportion of the islands' areas affected by low statistical significance (below 90 % based on the Mann-Kendall test). The low statistical significance in terms of precipitation trends in the Canary Islands has been commented on in previous

Table 8
Period of study (by start and end year). Sites by island with decadal precipitation trends statistically greater than 90% in mm/decade units.

Island	Trend start year	Trend end year	Total no. of years	Recorded precipitation decrease and zone (mm/decade)	Recorded precipitation increase and zone (mm/decade)
La Palma	1986	2020	35	−20 for mountainous areas of Cumbre Vieja, −10 for coastal areas in the S	+15 for the N coast of Don Pedro and Los Franceses
La Gomera	1980	2020	41	−10 in small areas in the centre of the island	Not observed
El Hierro	1991	2020	30	Not observed	+10 in the W and N tip in Guarazoca and Las Puntas
Tenerife	1986	2020	35	−10 for the SW and the triangular area Vilaflor-Arona-La Quinta, for the E between Granadilla and Las Vegas, area between Arafo and El Gaitero	+5 for Teno (NW), Santa Cruz-Taco (E)
Gran Canaria	1970	2020	51	−2 in small areas in the east coast (Gando airport and Carrizal) and in the southwest coast (Tauro and Puerto Rico)	Not observed
Fuerteventura	1970	2020	51	−2 in almost all the island except the southeast (Gran Tarajal area) and small areas in the centre and in the northeast (Corralejo)	Not observed
Lanzarote	1970	2020	51	Not observed	Not observed

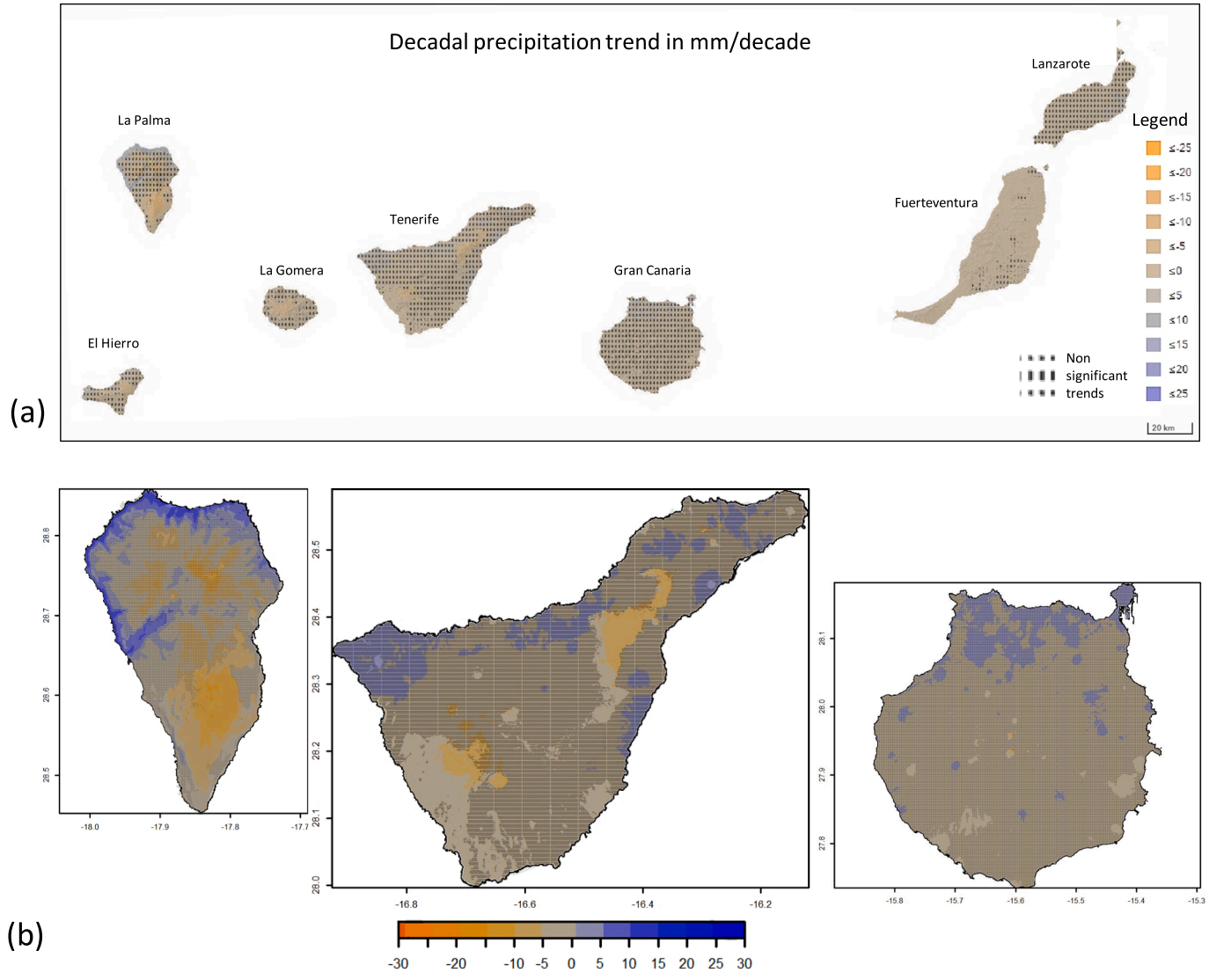

Fig. 14. Decadal precipitation trend map in mm/decade for (a) The different islands of the Canarian Archipelago in a 100 m spatial resolution map, (b) The most populated islands zoomed: from left to right La Palma, Tenerife and Gran Canaria.

publications (Dorta et al., 2018). Except for the island of Fuerteventura, with 68 % of its surface free of this low significance, the rest of the islands are highly affected, especially Gran Canaria and Lanzarote (see Fig. 14(a)). In Table 8, which shows the trend areas with statistical significances above 90 %, a predominance of areas with a decreasing precipitation trend can be observed, ranging between −2 and −20 mm/decade. These downward trends in the Canary Islands have also been observed in previous studies (Hernández et al., 2012; Máyer et al., 2017). Although the sites shown in Table 8 are irregularly distributed, three areas stand out for their extension, the Cumbre Vieja area to the south of La Palma and 2 woodland areas to the southwest and northeast of Tenerife. These 3 areas are clearly visible in Fig. 14(b), marked with

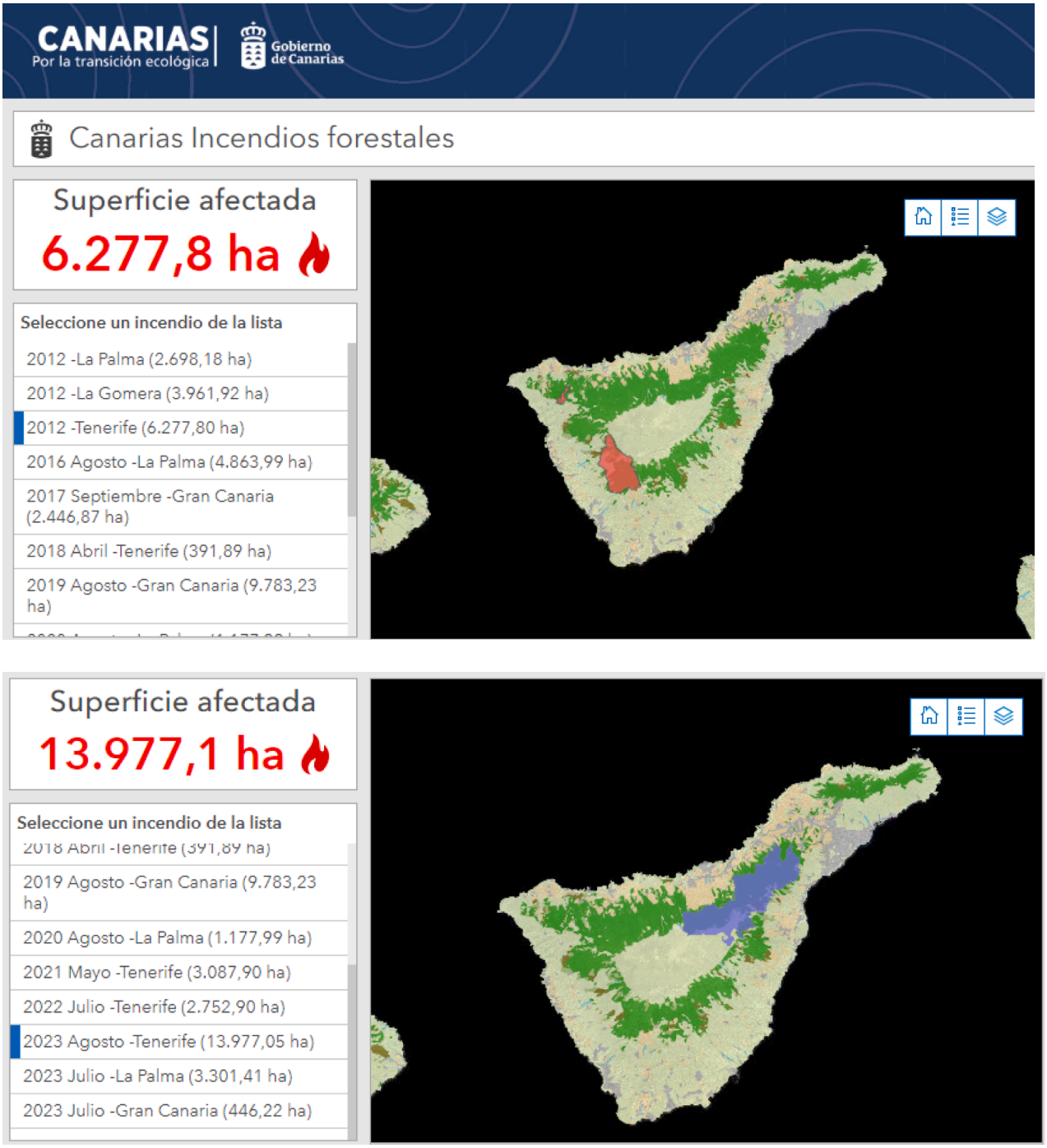

Fig. 15. Information about devastating fires in Tenerife obtained from the SITCAN database supported by the Canary Islands Government. The green colours on the slopes of the island show the woodland areas. (For interpretation of the references to colour in this figure legend, the reader is referred to the web version of this article.)

brown-orange tones.

Climate trend information as described in this study can serve to develop other useful maps for citizen security. For example, the climate variables of air temperature, precipitation, relative humidity and wind are used to generate wildfire risk maps. This is of particular importance in the islands given that a new type of wildfire has been observed in the last 15 years with very fast propagation and spreading over large areas (more than 5,000 ha). The two areas in Tenerife with negative precipitation trends (shown in Fig. 14(b) and highlighted in the previous paragraph) coincide with areas with positive temperature trends (shown in Fig. 13(a)) and, as they are woodland areas, have a high wildfire risk.

The SITCAN database on forest fires developed by the Canary Islands Government (SITCAN, 2023) shows information about the most devastating fires of the last 15 years in the Canary Islands. Fig. 15 shows information extracted from the database indicating two of these fires affecting the two aforementioned woodland areas in Tenerife. The first occurred in the southwest of the island in 2012, affecting 6,278 ha, and the second in August 2023, affecting 13,977 ha. Therefore, air temperature and precipitation trend maps seem to be useful to define and improve wildfire risk maps in the islands.

6. Conclusions

The ACDIC offers free and quick web access to different climate maps and data of the Canary Islands (https://atlasclimatico.sitcan.es/). It is the result of an effort to compile and statistically process climate data obtained from different national, regional and island institutions and organisations, as well as other data from satellite-based products and reanalyses. One of the main contributions of this atlas is the map- and chart-based visualisation of different variables, with the possibility of identifying the values of these variables in any part of the different island territories and contrasting the real and theoretical values obtained from the models at each point where there are observations. Another key aspect is the implementation of these maps at high spatial resolution given the significant impact of altitude and relief orientation on the different climatic variables and on the generation of the different topoclimates present on the islands.

The ACDIC has the advantage of being able to incorporate new products in the coming years, especially those related to climate change, making it a dynamic tool that can be constantly improved and updated. In this first version, it has not been possible to include useful variables to assess multiple aspects such as global solar radiation maps and potential evapotranspiration maps. In addition, and as mentioned, climate projections for different climate change scenarios should be included based on the 6th IPCC report (maps of annual and seasonal precipitation and temperature anomalies) for different scenarios (SSP1-2.6 to SSP5-8.5, where SSP are the Shared Socioeconomic Pathways) and time horizons (2040, 2060, 2080 and 2100). In this case, forward-looking models will be used with the highest possible spatial resolution (around 1 km) in order to identify in detail the areas affected by precipitation and temperature anomalies every 20 years. Diverse climate change indices can also be incorporated at different times.

CRediT authorship contribution statement

Ángel Luis de Luque Söllheim: Conceptualization, Data curation, Formal analysis, Investigation, Methodology, Software, Supervision, Validation, Visualization, Writing – original draft, Writing – review & editing. **Pablo Máyer Suarez:** Conceptualization, Data curation, Formal analysis, Funding acquisition, Investigation, Methodology, Project administration, Resources, Supervision, Validation, Visualization, Writing – review & editing. **Fabián García Hernández:** Data curation, Methodology.

Declaration of competing interest

The authors declare that they have no known competing financial interests or personal relationships that could have appeared to influence the work reported in this paper.

Data availability

The original data from the weather stations belong to the institutions that provided them. The created climate maps can be viewed and downloaded via the web and the code can be requested by email.

Acknowledgements

This work would not have been possible without the work carried out for decades by public agencies responsible for the management of meteorological observation networks, as well as by the observers who, over these years, have worked anonymously in the collection of these instrumental data for climatic purposes. The following organizations are cited:

- Climatology Section of the Eastern Canary Centre of the State Meteorological Agency of Spain (AEMET by its initials in Spanish).
- To the Island Council of La Palma, the AgroCouncil network of Tenerife Island Council, and the Water Boards of the Island Councils of Gran Canaria, Fuerteventura and Lanzarote.
- To the managers of the networks of the Agroclimatic Information System for Irrigation (SIAR by its initials in Spanish) and the Canarian Institute of Agricultural Research (ICIA by its initials in Spanish).

The Interactive Climate Atlas Project of the Canary Islands was developed under an institutional collaboration agreement for the Improvement of Climate and Climate Change Information in the Canary Islands, signed in December 2020 between the University of Las Palmas de Gran Canaria and the Ministry of Ecological Transition, Fight against Climate Change and Territorial Planning of the Government of the Canary Islands and included in the budget of the Autonomous Community of the Canary Islands.

References

AEMET, 2012. Climate atlas of the archipelagos of the Canary Islands, Madeira and the Azores. The Meteorological State Agency of Spain and the Institute of Meteorology, Portugal. https://www.aemet.es/documentos/es/conocermas/recursos_en_linea/publicaciones_y_estudios/publicaciones/2Atlas_climatologico/Atlas_Clima_Macaronesia__Baja.pdf.

Agnew, M.D., Palutikof, J.P., 2000. GIS-based construction of base line climatologies for the Mediterranean using terrain variables. Climate Res. 14, 115–127.

Alexandersson, H., 1986. A homogeneity test applied to precipitation data. J. Climatol. 6, 661–675.

Antolović, I., Mihajlović, V., Rančić, D., Mihić, D., Djurdjević, V., 2013. Digital climate atlas of the carpathian region. Adv. Sci. Res. 10, 107–111. https://doi.org/10.5194/asr-10-107-2013.

Brown, D.P., Comrie, A.C., 2002. Spatial modeling of winter temperature and precipitation in Arizona and New Mexico, USA. Climate Res. 22, 115–128.

Cohen, J., Cohen, P., West, S., Aiken, L., 2003. Applied multiple regression/correlation analysis for the behavioural sciences, Lawrence Erlbaum, 0805822232.

Copernicus Climate Change Service, Climate Data Store, 2019. UERRA regional reanalysis for Europe on pressure levels from 1961 to 2019. Copernicus Climate Change Service (C3S) Climate Data Store (CDS). https://doi.org/10.24381/cds.92221551 (Accessed on 01-MAR-2023).

Copernicus Climate Change Service, Climate Data Store, 2019. UERRA regional reanalysis for Europe on single levels from 1961 to 2019. Copernicus Climate Change Service (C3S) Climate Data Store (CDS). https://doi.org/10.24381/cds.32b04ec5 (Accessed on 01-MAR-2023).

Cortesi, N., Gonzalez-Hidalgo, J.C., Brunetti, M., Martin-Vide, J., 2012. Daily precipitation concentration across Europe 1971–2010. Nat. Hazards Earth Syst. Sci. 12, 2799–2810. https://doi.org/10.5194/nhess-12-2799-2012.

Cropper, T.E., Hanna, E., 2013. An analysis of the climate of Macaronesia, 1865–2012. Int. J. Climatol. 34, 604–622. https://doi.org/10.1002/joc.3710.

Daly, C., 2006. Guidelines for assessing the suitability of spatial climate data sets. Int. J. Climatol. 26, 707–721.

Daly, C., Gibson, W.P., Taylor, G.H., Johnson, G.L., Pasteris, P., 2002. A knowledge-based approach to the statistical mapping of climate. Clim Res 22, 99–113.

Dorta Antequera, P., 1996. Las inversiones térmicas en Canarias. Investigaciones Geográficas. 15, 109–124. https://doi.org/10.14198/INGEO1996.15.01.

Dorta, P., Díez, A.L., Pacheco, J.D., 2018. El calentamiento global en el Atlántico Norte Suroriental. El caso de Canarias. Estado de la cuestión y perspectivas de futuro. Cuadernos geográficos de la Universidad de Granada 57 (2), 27–52.

Fernández, A., Romero, R., Zavala, J., 2014. Methodologies used in the digital climatic atlas of Mexico for generating high-resolution maps. Geoacta 39, n.1.

Fick, S.E., Hijmans, R.J., 2017. WorldClim 2: new 1km spatial resolution climate surfaces for global land areas. Int. J. Climatol. 37 (12), 4302–4315.

Giambelluca, T.W., Shuai X., Barnes M.L., Alliss R.J., Longman R.J., Miura T., Chen Q., Frazier A.G., Mudd R.G., Cuo L., & Businger A.D., 2014. Evapotranspiration of Hawai'i. Final report submitted to the U.S. Army Corps of Engineers—Honolulu District, and the Commission on Water Resource Management, State of Hawai'i.

Goovaerts, P., 1999. Using elevation to aid the geostatistical mapping of rainfall erosivity. Catena 34, 227–242.

Guijarro, J.A., López, J.A., Aguilar, E., Domonkos, P., Venema, V.K.C., Sigró, J., Brunet, M., 2023. Homogenization of monthly series of temperature and precipitation: Benchmarking results of the MULTITEST project. Int. J. Climatol. 43 (9), 3994–4012. https://doi.org/10.1002/joc.8069.

Guijarro, J.A., 2023. User guide for the R package climatol (version 4.0.7). https://www.climatol.eu/climatol4-en.pdf.

Guttman, N.B., Quayle, R., 1990. A review of cooperative temperature data validation. J. Atmos. Oceanic Technol. 7, 334–339.

Harris, I., Jones, P.D., Osborn, T.J., Lister, D.H., 2014. Updated high-resolution grids of monthly climatic observations - the CRU TS3.10 Dataset. Int. J. Climatol. 34, 623–642. https://doi.org/10.1002/joc.3711.

Hernández, S., Tarife, R., Gámiz, R., Castro, Y. & Esteban, M.J., 2012. Estudio de las sequías en las Islas Canarias mediante el análisis de índices multiescalares. (Eds.)

cambio climático, Extremos e impactos. Asociación Española de Climatología, Serie A, 8, 421-430.
Hession, S.L., Moore, N., 2011. A spatial regression analysis of the influence of topography on monthly rainfall in East Africa. Int. J. Climatol. 31, 1440–1456.
Huade, G., Wilson, J.L., Makhnin, O., 2005. Geostatistical mapping of mountain precipitation incorporating autosearched effects of terrain and climatic characteristics. J. Hydrometeorol. 6, 1018–1031.
Inspire, 2007. Directive of the European Parliament and of the Council of 14. March 2007 Establishing an Infrastructure for Spatial Information in the European Community (INSPIRE).
Iturbide, M., Fernández, J., Gutiérrez, J.M., Bedia, J., Cimadevilla, E., Díez-Sierra, J., Manzanas, R., Casanueva, A., Baño-Medina, J., Milovac, J., Herrera, S., Cofiño, A.S., San Martín, D., García-Díez, M., Hauser, M., Huard, D., Yelekci, Ö., 2021. Repository supporting the implementation of FAIR principles in the IPCC-WG1 Atlas. Zenodo. https://doi.org/10.5281/zenodo.3691645. Available from: https://github.com/IPCC-WG1/Atlas.
Kendall, M.G., 1975. Rank correlation methods. Griffin, London.
Khaliq, M.N., Ouarda, T.B.M.J., 2007. On the critical values of the standard normal homogeneity test (SNHT). Int. J. Climatol. 27, 681687.
Kottek, M., Grieser, J., Beck, C., Rudolf, B., Rubel, F., 2006. World Map of the Köppen-Geiger climate classification updated. Meteorol. z. 15, 259–263. https://doi.org/10.1127/0941-2948/2006/0130.
Liu, R., Liu, Y., 2013. Generation of new cloud masks from MODIS land surface reflectance products. Remote Sens. Environ. 133, 21–37. https://doi.org/10.1016/j.rse.2013.01.019.
López Gómez, J., López, G.A., 1979. El clima de Canarias según la clasificación de Köppen. Estudios Geográficos 156, 321–340.
Luque, A., Martín, J.L., Dorta, P., Mayer, P., 2014. Temperature trends on gran canaria (Canary Islands). an example of global warming over the subtropical northeastern atlantic. Atmospheric Clim. Sci.
Mann, H.B., 1945. Nonparametric tests against trend. Econometria 13, 245–259. https://doi.org/10.1002/joc.870.
Marquínez, J., Lastra, J., García, P., 2003. Estimation models for precipitation in mountainous regions: the use of GIS and multivariate analysis. J. Hydrol. 270, 1–11.
Martín, J.L., Bethencourt, J., Cuevas-Agulló, E., 2012. Assessment of global warming on the island of Tenerife, Canary Islands (Spain). Trends in minimum, maximum and mean temperatures since 1944. Clim. Change 114, 343–355.
Marzol, MV., Máyer, P., 2012. Algunas reflexiones acerca del clima de las islas Canarias. Nimbus 29-30, 399–416.
Máyer, P., Marzol, M. and Parreño, J. 2017. Precipitation trends and a daily precipitation concentration index for the mid-Eastern Atlantic (Canary Islands, Spain). Cuadernos de Investigación Geográfica. 43, 1 (Jun. 2017), 255–268. https://doi.org/10.18172/cig.3095.
Muñoz Sabater, J., 2019. ERA5-Land monthly averaged data from 1950 to present. Copernicus Climate Change Service (C3S) Climate Data Store (CDS). https://doi.org/10.24381/cds.68d2bb30 (Accessed on 20-MAY-2022).
Ninyerola M., Pons X. & Roure J.M., 2005. Atlas Climático Digital de la Península Ibérica. Metodología y aplicaciones en bioclimatología y geobotánica. © Universidad Autónoma de Barcelona. (DL: B-42538-2005, ISBN: 932860-8-7) (http://opengis.uab.es/wms/iberia/).
Morales, G., Pérez-González, R., 2000. Gran atlas temático de Canarias. Editorial Interinsular Canaria.
Ninyerola, M., Pons, X., Roure, J.M., 2000. A methodological approach of climatological modelling of air temperature and precipitation through GIS techniques. Int. J. Climatol. 20, 1823–1841.
Nuñez Lopez, D., Treviño Garza, E., Reyes Gomez, V., Muñoz Robles, C., Aguirre Calderón, O., Jiménez Pérez, J., 2014. Uso de modelos de regresión para interpolar espacialmente la precipitación media mensual en la cuenca del rio Conchos. Revista Mexicana De Ciencias Agrícolas 5 (2), 201–213.
Prudhomme, C., Reed, D.W., 1998. Relationships between extreme daily precipitation and topography in a mountainous region: a case study in Scotland. Int. J. Climatol. 18, 1439–1453.
Raso Nadal J. M., P. Clavero Paricio and J. Martín Vide. 1984, Distribución probabilística de la precipitación anual en Cataluña. Revista de Geografía. Vol XVIII. Barcelona. pp 47-68.
Sen, P.K., 1968. Estimates of the regression coefficient based on Kendall's Tau. J. Am. Stat. Assoc. 63, 1379–1389.
SITCAN, 2023. Territorial Information System of the Canary Islands, forest fires section. https://servicios.sitcan.es/portal/apps/experiencebuilder/experience/?id=362b7b2072884162a785857f86e14eeb&page=page_6 (accessed 20 December 2023).
Theil, H., 1950. A Rank-Invariant Method of Linear and Polynomial Regression Analysis, I-III. Proc. Kon. Ned. Akad. v. Wetensch. A. 53, 386-392, 521-525, 1397-1412.
Vicente-Serrano, S.M., Saz-Sánchez, M.A., Cuadrat, J.M., 2003. Comparative analysis of interpolation methods in the middle Ebro Valley (Spain): application to annual precipitation and temperature. Climate Res. 24, 161–180.
Wilson, A.M., Jetz, W., 2016. Remotely sensed high-resolution global cloud dynamics for predicting ecosystem and biodiversity distributions. PLoS Biol. 14 (3), e1002415.